Supporting Information

Late-Stage Microsomal Oxidation Reduces Drug-Drug Interaction and Identifies Phosphodiesterase 2A Inhibitor PF-06815189

Antonia F. Stepan,† Tuan P. Tran,‡ Christopher J. Helal,‡ Maria Brown,‡ Cheng Chang,‡ Rebecca E. O'Connor,‡ Michael De Vivo,† Shawn D. Doran,‡ Ethan L. Fisher,‡ Stephen Jenkinson,§ David Karanian,‡ Bethany L. Kormos,† Raman Sharma,‡ Gregory S. Walker,‡ Ann S. Wright,‡ Edward X. Yang,‡ Michael A. Brodney,† Travis T. Wager,† Patrick R. Verhoest,† R. Scott Obach‡*

†Pfizer Worldwide Research and Development, 610 Main Street, Cambridge, Massachusetts 02139, United States
‡Pfizer Worldwide Research and Development, Eastern Point Road, Groton, Connecticut 06340, United States
§Pfizer Worldwide Research and Development, 10770 Science Center Drive, La Jolla, California 92121, United States

Content

Dihedral angle calculation for 1

Dihedral angle scans on the bond that connects the imidazotriazinone core with the dimethylpyrazole substituent (defined in Figure S-1) were performed on **1** with and without the methyl at the 3-position on the pyrazole; the results suggested that this methyl has an effect on the orientation of the pyrazole substituent (Figure S-1). The docked pose (i.e. bound conformation) of **1** in PDE2 has a dihedral angle of 66°, in alignment with the 67° dihedral angle observed in the X-ray crystal structure of a related compound.[1] The local minimum energy structure of **1** has a dihedral angle of 45°, while that of compound Z (**cmpd Z)** has a dihedral angle of 0.0°. This suggests that the 3-methyl on the pyrazole ring causes the phenyl ring to adopt a conformation that is closer to the bound conformation, leading to a smaller conformational energy penalty upon binding. In addition, optimization of the compounds indicate that the conformational strain energy required to achieve the bound conformation without a 3-methyl on the pyrazole, ~3.0 kcal/mol, may be 3x that of those with a methyl on the pyrazole, ~0.9 kcal/mol.

Compound	Conformational Strain (kcal/mol)
1	0.87
cmpd Z	3.06

Computational Methods

Dihedral angle scans were performed on **1** and **cmpd Z** on the bond that connects the imidazotriazinone core with the dimethylpyrazole substituent. The dihedral angle was increased from 0° to 360° in increments of 10° and each resultant structure was optimized at the B3LYP-D3/6-31+G** level of theory[2] followed by single-point energy calculations at the M06-2X/cc-PVDZ level of theory[3] in Jaguar (version 9.4, Schrödinger, LLC, New York, NY, 2016).[4] Conformational strain energies were calculated as follows: 1) **1** and **cmpd Z** were docked into the PDE2 X-ray co-crystal structure with **BAY 60-7550**[5] using Glide (Schrödinger, LLC, New York, NY, 2016)[6] in standard precision (SP) mode with default parameters following protein preparation (Schrödinger Suite 2016-4 Protein Preparation Wizard; Epik, Schrödinger, LLC, New York, NY, 2016; Impact, Schrödinger, LLC, New York, NY, 2016; Prime, Schrödinger, LLC, New York, NY, 2016)[7] with default parameters and grid generation using **BAY 60-7550** to define the site, 2) the dihedral angle was adjusted to the optimal angle from the DFT scan (40° and 0° for **1** and **cmpd Z**, respectively) or constrained to the angle in the bound conformation generated from docking (66°), and 3) the energies were calculated at the M06-2X/cc-PVDZ//B3LYP-D3/6-31+G** level of theory. Conformational energy penalties were estimated by subtracting the relative energy at the local minima dihedral angle for **1** and **cmpd Z** from their respective energies at the dihedral angle of the bound conformation.

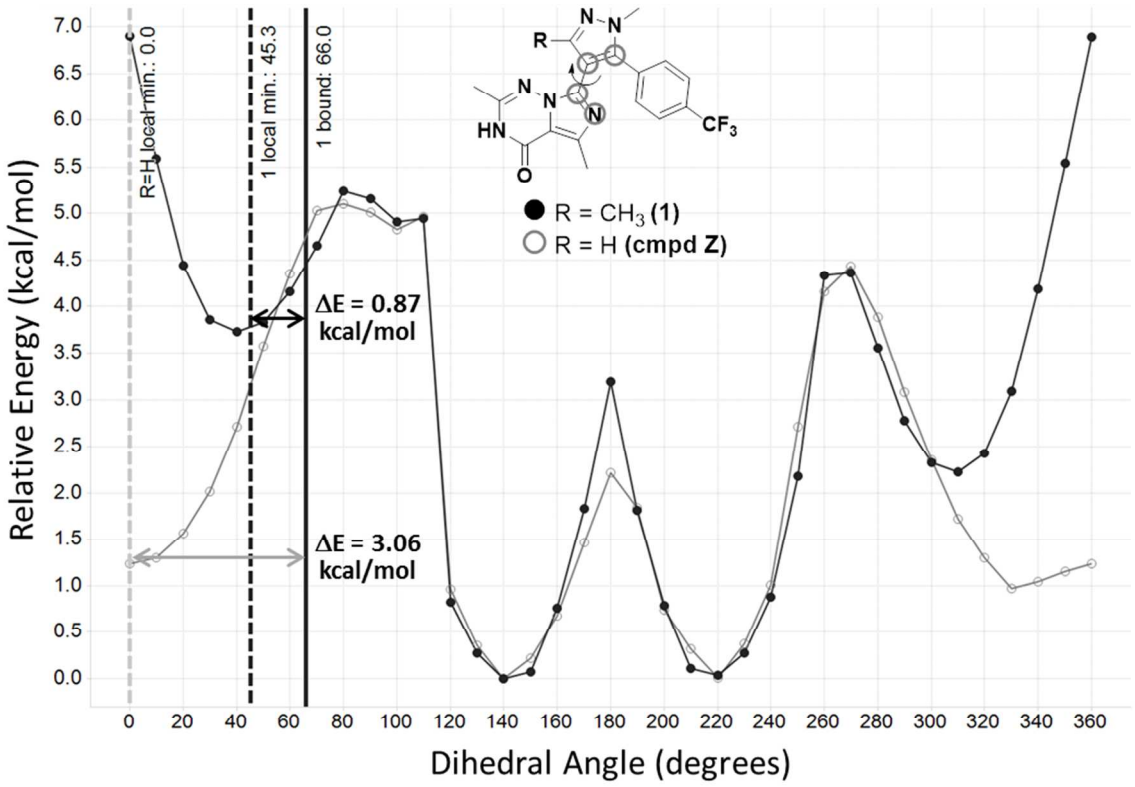

Figure S-1. **Relative energies from dihedral scan with 1 and its des-methyl analog cmpd Z.**

Procedure for testing the effectiveness of liver microsomal samples from several species and panel of heterologously expressed common human P450 enzymes at metabolizing 1 (see Figures S-2 and S-3)

In an initial screen, **1** (20 μM) was incubated with liver microsomes from several species (2 mg/mL; sourced from either Corning-Gentest, Woburn, MA, Xenotech, Lenexa, KS, or prepared in-house) as well as several human P450 enzymes (at varying concentrations of P450; Corning-Gentest, Woburn, MA or PanVera, Madison, WI) in a volume of 0.5 mL of potassium phosphate buffer (100 mM, pH 7.4) containing $MgCl_2$ (3.3 mM) and NADPH (1.3 mM). Incubations were carried out at 37 ^oC for 50 min followed by addition of CH_3CN (2.5 mL) to terminate the reaction and precipitate the protein. Following centrifugation at 1700 g for 5 min, the supernatants were evaporated in a vacuum centrifuge and the residues were reconstituted in 1% HCOOH in water (0.1 mL). Injections (10 μL) were made on a Waters Acquity HSS T3 C18 column (2.1 x 100 mm; 1.8 μ) equilibrated in 0.1% HCOOH in 10% CH_3CN at a flow rate of 0.35 mL/min. This mobile phase composition was maintained for 0.5 min followed by a linear gradient to 35% CH_3CN at 5.5 min, a second gradient to 80% CH_3CN at 9 min, 1 min of column washing at 95% CH_3CN, and a 1.5 min re-equilibration. The eluent flowed through a photodiode array UV/VIS detector (200-400 nm) and into the ion source of a Thermo Orbitrap Elite high resolution mass spectrometer operated in the positive ion mode. Mass spectrometer source potentials and temperatures, as well as collision energies in the ion trap were adjusted to optimize for the signal and fragmentation of **1**.

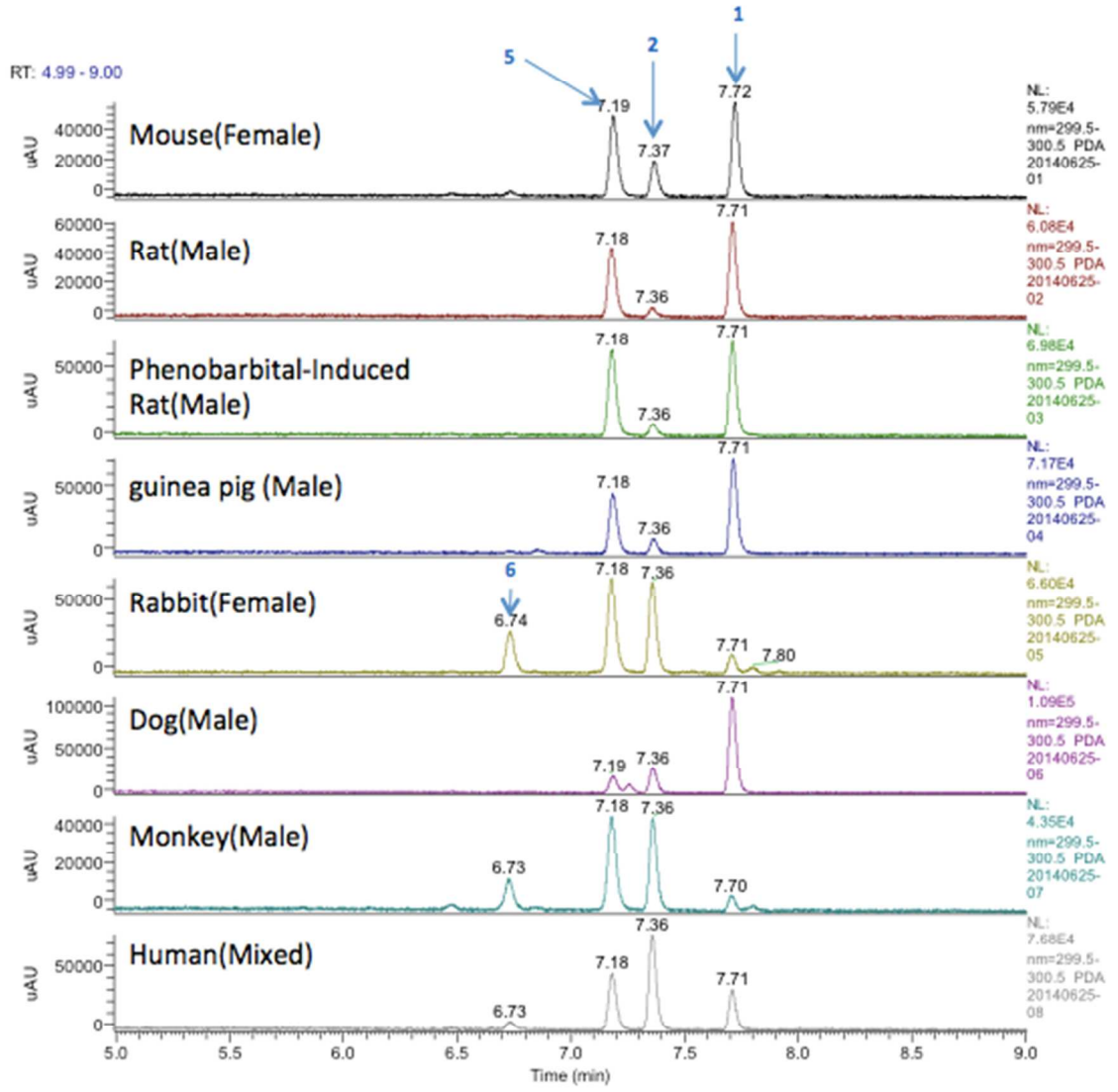

Figure S-2. UHPLC-UV Chromatograms of Compound **1** Incubation Extracts from Liver Microsomes of various species. The wavelength is 300 nm. Retention times for **1**, PF-06815189 (**2**), **5**, and **6** were 7.7, 7.4, 7.2, and 6.7 min, respectively. The most effective enzyme sources for the generation of all three compounds were the rabbit and the monkey. The monkey was selected for scaling the biosynthesis incubation.

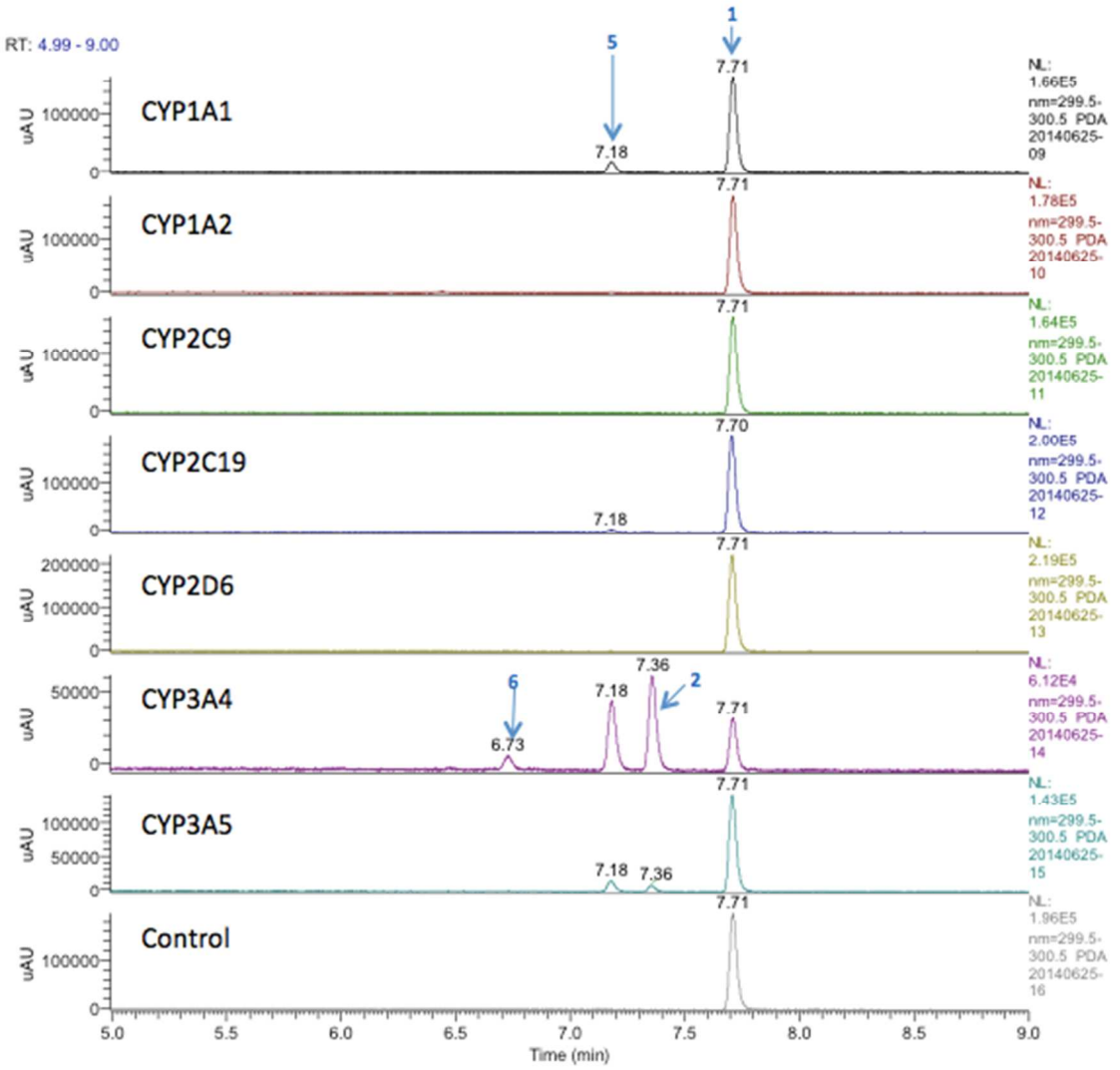

Figure S-3. UHPLC-UV Chromatograms of Compound **1** Incubation Extracts from Expressed Human P450 Enzymes. The wavelength is 300 nm. Retention times for **1**, PF-06815189 (**2**), **5**, and **6** were 7.7, 7.4, 7.2, and 6.7 min, respectively. This work was done to understand the type of CYP enzyme responsible for the oxidation of compound **1** by human liver microsomes and it was found that the most effective enzyme source for the generation of all three compounds was CYP3A4.

Procedure for synthesis of PF-06815189, 5 and 6 using monkey liver microsomal incubation

Monkey liver microsomes (2 mg/mL; Corning-Gentest, Woburn, MA) were utilized, the concentration of **1** was 30 μM, the incubation volume was 20 mL, and the incubation time was 40 min. At the end of the incubation, CH_3CN (20 mL) was added and the precipitated material was removed by centrifugation (5 min; 1700 g). The supernatant was subjected to vacuum centrifugation for 1 hr to remove the CH_3CN and to the remaining material was added formic acid (0.5 mL) and water to a total volume of 50 mL. This mixture was spun in a centrifuge for 30 min (40000 g) and the supernatant was applied to a Polaris C18 column (4.6 x 250 mm; 5 μ) at 0.8 mL/min through a Jasco HPLC pump. After loading this material, the column was moved to an HPLC-MS system in line with a fraction collector. The metabolites were eluted with a gradient starting at 2% CH_3CN in 0.1% HCOOH, immediately raised to 10% CH_3CN, held for 5 min, and raised to 60% CH_3CN at 75 min. The flow rate was 0.8 mL/min and the eluent was split between the mass spectrometer and fraction collector at a ratio of approximately 1:20. Fraction were collected every 20 sec. Fractions collected at times approximate to where peaks of interest eluted (i.e. having *m/z* values demonstrating that they are related to **1**) were checked for identity and purity using the UHPLC-HRMS system described above. Fractions were pooled as appropriate and the solvent was removed by vacuum centrifugation for analysis by NMR spectroscopy. Yields: Compound PF-06895189: 21%, compound **5**: 38%, compound **6**: 3.5%.

Metabolism of 1 in Monkey Liver Microsomes

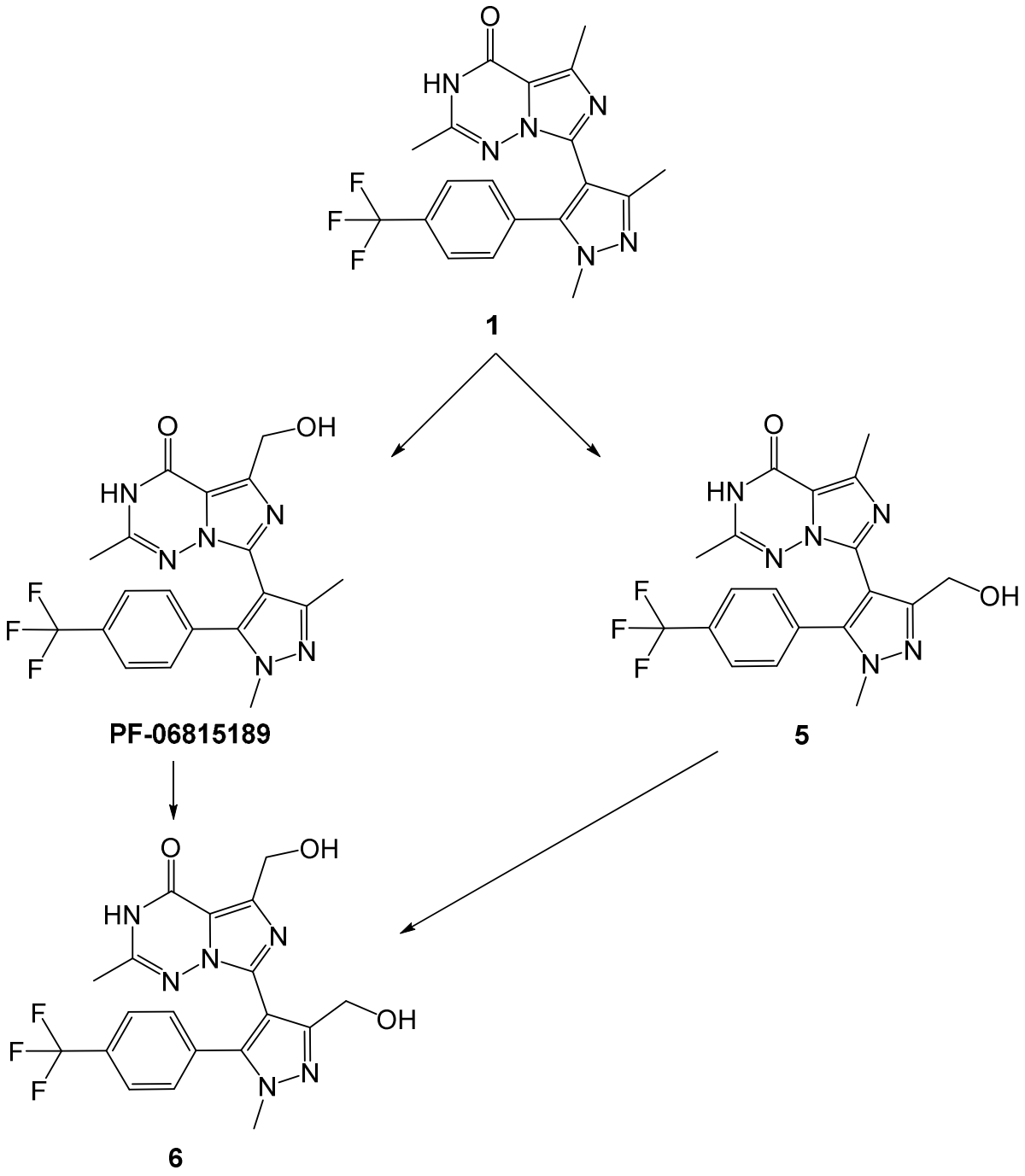

High resolution mass spectra of PF-06815189, 5 and 6 obtained from the monkey liver microsomal incubation

High Resolution Mass Spectrum for PF-06815189

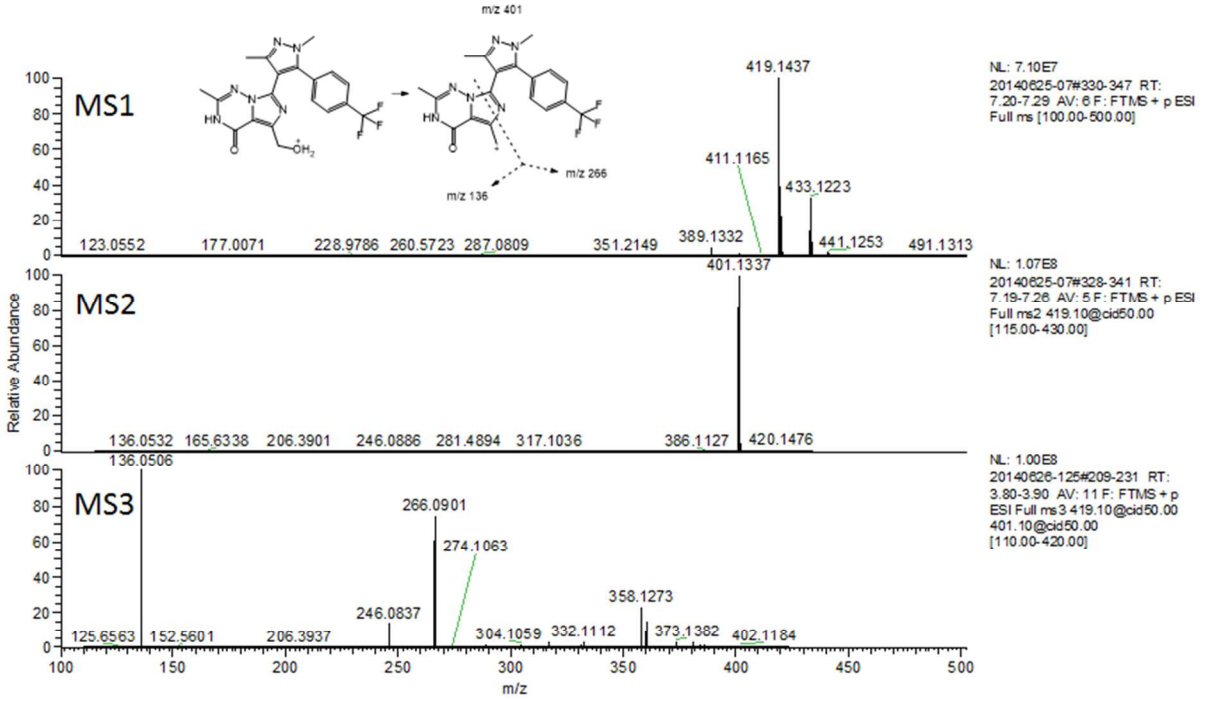

High Resolution Mass Spectrum for **5**

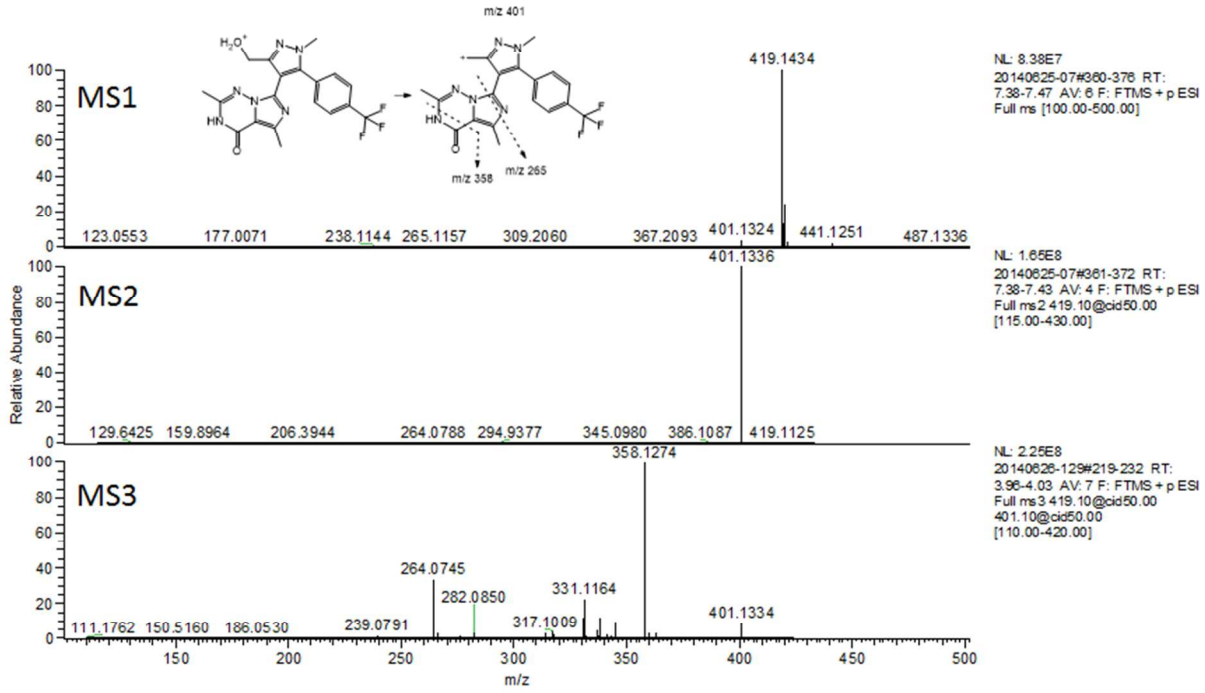

High Resolution Mass Spectrum for Compound **6**

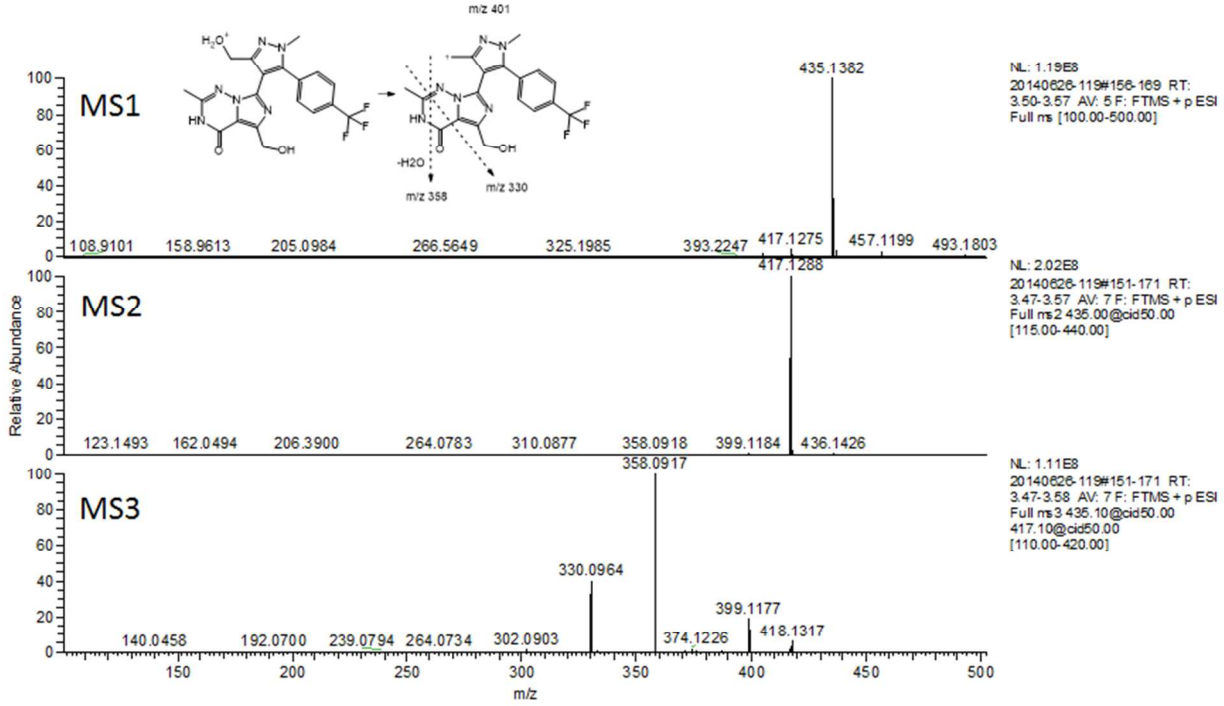

NMR Characterization of PF-06815189, 5 and 6 obtained from the monkey liver microsomal incubation

NMR Methods

All samples were dissolved DMSO-d6 "100%" and placed in a 1.7 mm NMR tube (0.04 ml isolated materials) or a 3 mm NMR tube (0.150 ml parent compound) under a dry argon atmosphere. ^{1}H and ^{13}C spectra were referenced using residual DMSO-d6 (^{1}H δ=2.50 ppm relative to TMS, δ=0.00, ^{13}C δ=39.50 ppm relative to TMS, δ=0.00). NMR spectra were recorded on a Bruker Avance 600 MHz (Bruker BioSpin Corporation, Billerica, MA) controlled by Topspin V3.2 and equipped with a 1.7 mm TCI Cryo probe (isolated materials) or a 5 mm BBFO cryo probe (parent compound). 1D spectra were recorded using an approximate sweep width of 8400 Hz and a total recycle time of approximately 7 s. 2D data were recorded using the standard pulse sequences provided by Bruker. Post-acquisition data processing was performed with either Topspin V3.2 or MestReNova V9.1 Quantitation of NMR isolates was performed by external calibration against the ^{1}H NMR spectrum of a 5 mM benzoic acid standard using the ERETIC2 function within Topspin V3.2.

NMR Assignments

Compound 1

The ^{1}H NMR of **1** has three aromatic resonances from five hydrogens; N4 - δ 11.46 (s, 1H), C22/24 - δ 7.77 (d, J = 8.2 Hz, 2H), C21/25 - δ 7.55 (d, J = 8.0 Hz, 2H),and twelve aliphatic hydrogens from four resonances; C19 - δ 3.80 (s, 3H),C12 - δ 2.45 (s, 3H), C18 - δ 2.21 (s, 3H) and C10 - δ 1.87 (s, 3H), Supplemental Figure NMR 1. The assignments for the resonances are supported by ^{1}H-^{13}C multiplicity edited HSQC, ^{1}H-^{13}C HMBC and ^{1}H-^{15}N HMBC, Supplemental Figures NMR 2, 3 and 4.

^{1}H NMR (600 MHz, DMSO-d_6) δ 11.46 (s, 1H), 7.77 (d, J = 8.2 Hz, 2H), 7.55 (d, J = 8.0 Hz, 2H), 3.80 (s, 3H), 2.45 (s, 3H), 2.21 (s, 3H), 1.87 (s, 3H).

Compound **1** Fraction 119/Compound 6

The ^{1}H NMR of **6** has three aromatic resonances from five hydrogens; N4 - δ 11.91 (bs, 1H), C22/24 - δ 7.78 (d, J = 8.0 Hz, 2H), C21/25 - δ 7.59 (d, J = 8.0 Hz, 2H),and twelve aliphatic hydrogens from five resonances; O30/31 - 5.25 (s, 2H) , C12 - 4.66 (d, J = 4.5 Hz, 2H), C18 - 4.51 (d, J = 5.2 Hz, 2H), C19 - δ 3.85 (s, 3H), and C10 - δ 1.82 (s, 3H), Supplemental Figure NMR 5. The assignments for the resonances are supported by ^{1}H-^{1}H COSY, ^{1}H-^{13}C multiplicity edited HSQC and ^{1}H-^{13}C HMBC, Supplemental Figures NMR 6, 7 and 8. The concentration of Compound **1** Fraction 119 (**6**), as determined by qNMR, was 0.44 mM.

^{1}H NMR (600 MHz, DMSO-d_6) δ 11.91 (bs, 1H), 7.78 (d, J = 8.0 Hz, 2H), 7.59 (d, J = 8.0 Hz, 2H), 5.25 (s, 2H), 4.66 (d, J = 4.5 Hz, 2H), 4.51 (d, J = 5.2 Hz, 2H), 3.85 (s, 3H), 1.82 (s, 3H).

Compound **1** Fraction 129/Compound **5**
The ^{1}H NMR of **5** has three aromatic resonances from five hydrogens; N4 - δ 11.47 (bs, 1H), C22/24 - δ 7.79 (d, J = 8.0 Hz, 2H), C21/25 - δ 7.57 (d, J = 8.0 Hz, 2H),and twelve aliphatic hydrogens from five resonances; O30 - 5.21 (s, 1H) , C18 - 4.50 (s, 2H), C19 - δ 3.84 (s, 3H), C12- δ 2.47 (s, 3H) and C10 - δ 1.82 (s, 3H), Supplemental Figure NMR 9. The assignments for the resonances are supported by ^{1}H-^{1}H COSY, ^{1}H-^{13}C multiplicity edited HSQC and ^{1}H-^{13}C HMBC, Supplemental Figures NMR 10, 11 and 12. The concentration of Compound **1** Fraction 129 (**5**), as determined by qNMR, was 1.9 mM.

^{1}H NMR (600 MHz, DMSO-d_6) δ 11.47 (s, 1H), 7.79 (d, J = 8.0 Hz, 2H), 7.57 (d, J = 8.0 Hz, 2H), 5.21 (s, 1H), 4.50 (s, 2H), 3.84 (s, 3H), 2.47 (s, 3H), 1.82 (s, 3H).

Compound **1** Fraction 125/PF-06815189
The concentration determined by qNMR was 1.8 mM. For compounds characterization, see the synthesis section 'Procedures for the large scale synthesis of **PF-06815189**'.

Supplemental NMR Figures

NMR 1 - The ^{1}H NMR of Compound **1**.

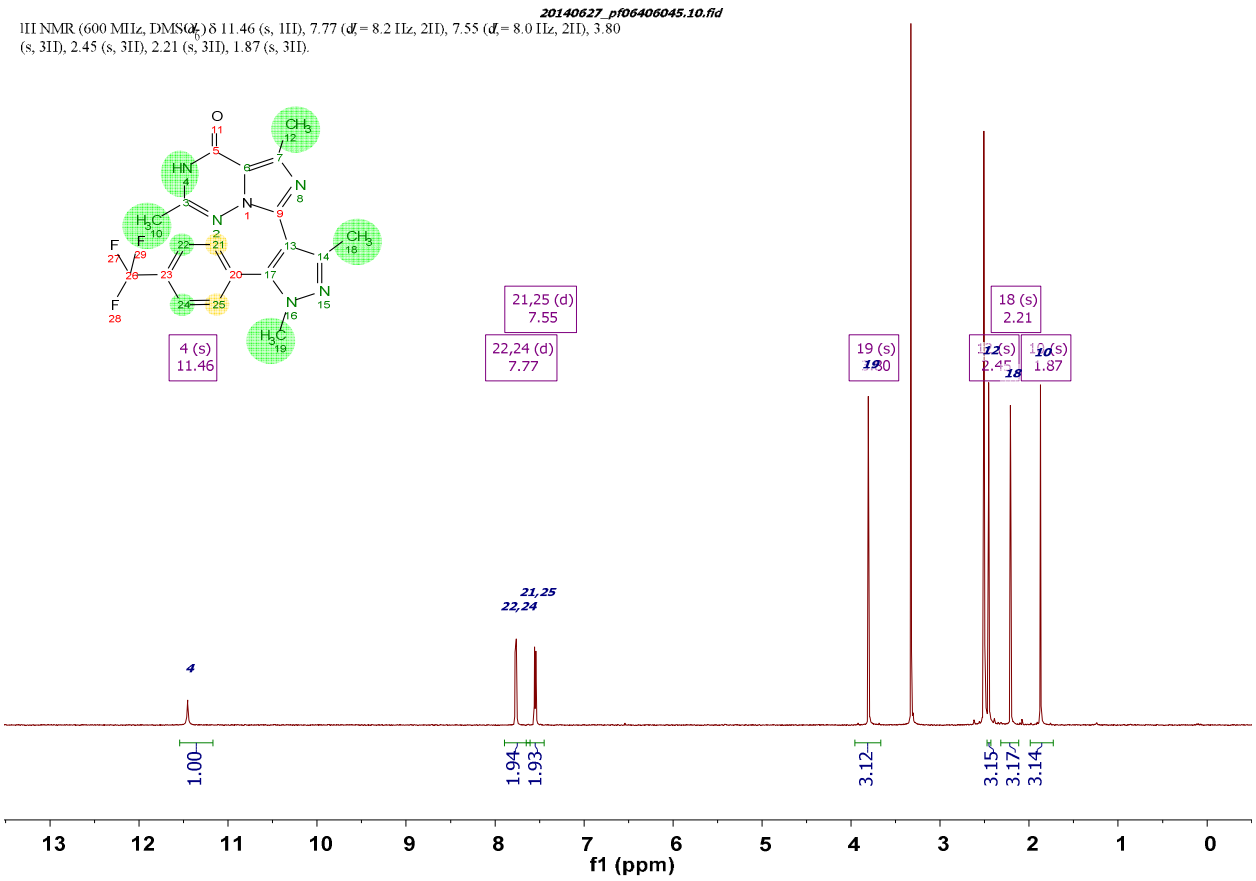

NMR2 The ^{1}H-^{13}C multiplicity edited HSQC of Compound **1**.

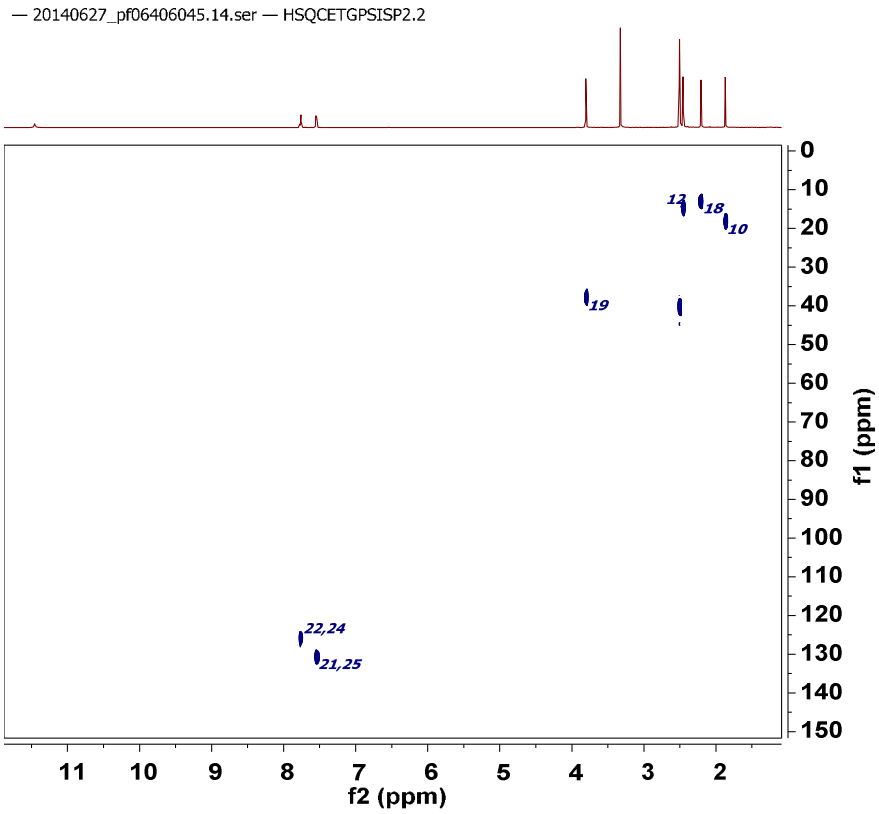

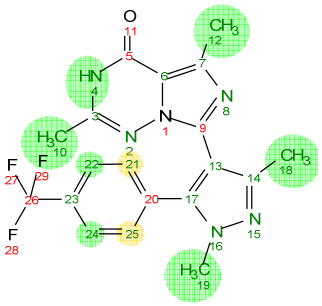

NMR3 The ^{1}H-^{13}C HMBC of Compound **1**

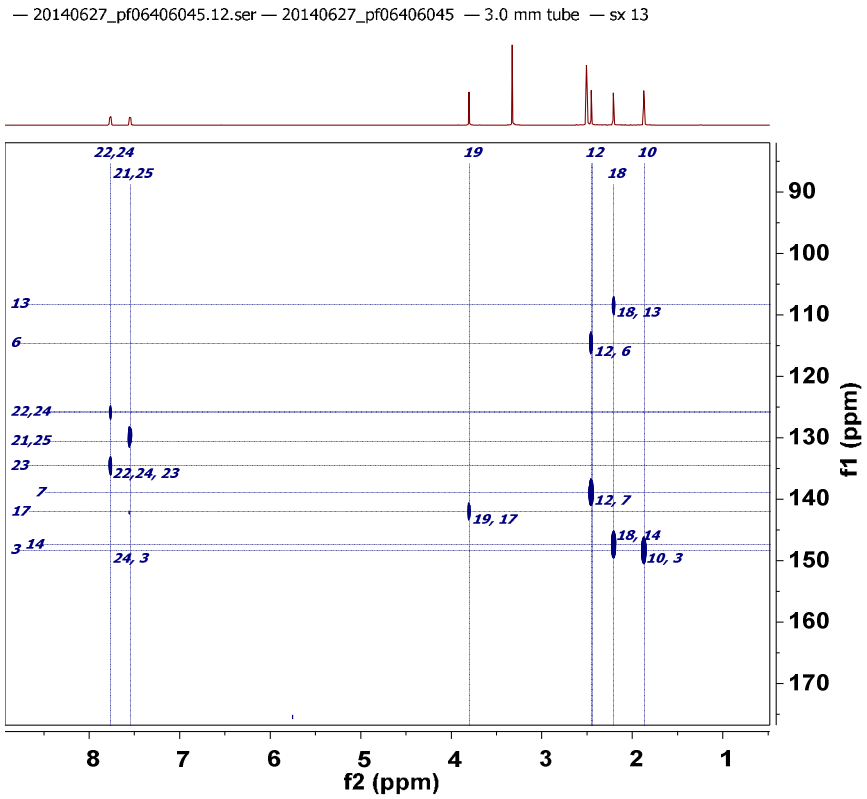

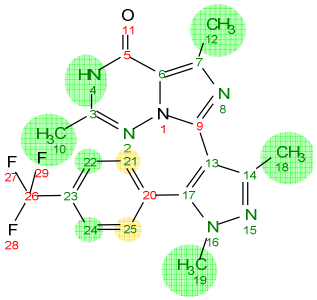

NMR4 The ^{1}H-^{15}N HMBC of Compound **1**

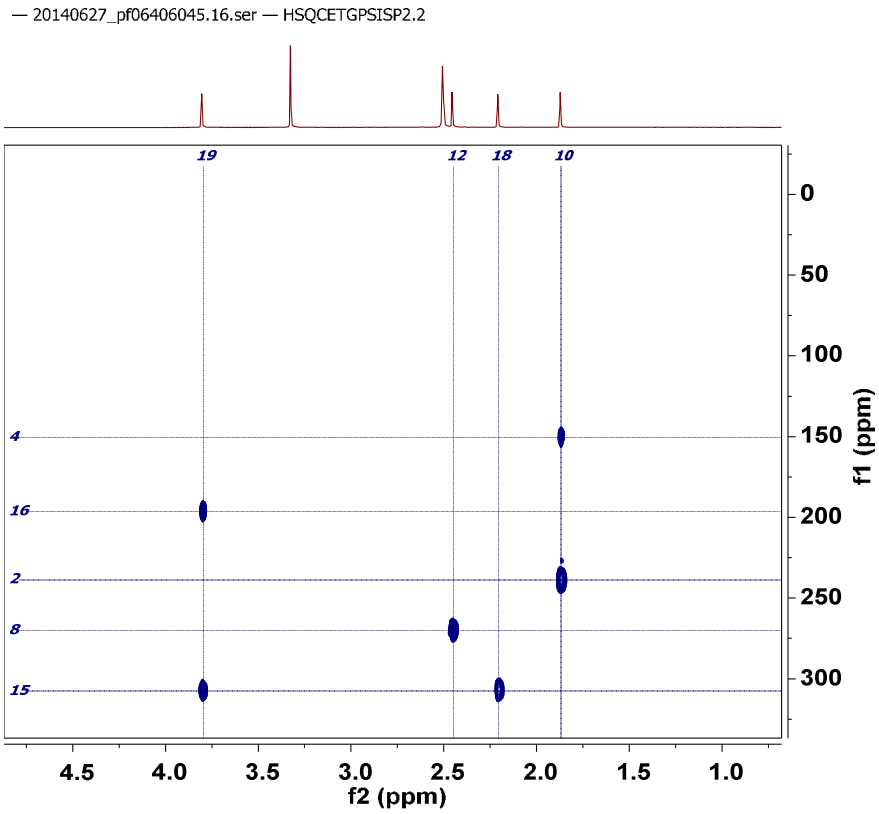

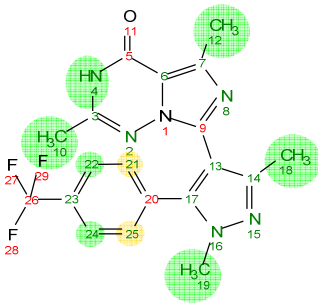

NMR5 The ^{1}H NMR of Compound **1** Fraction 119 (**6**).

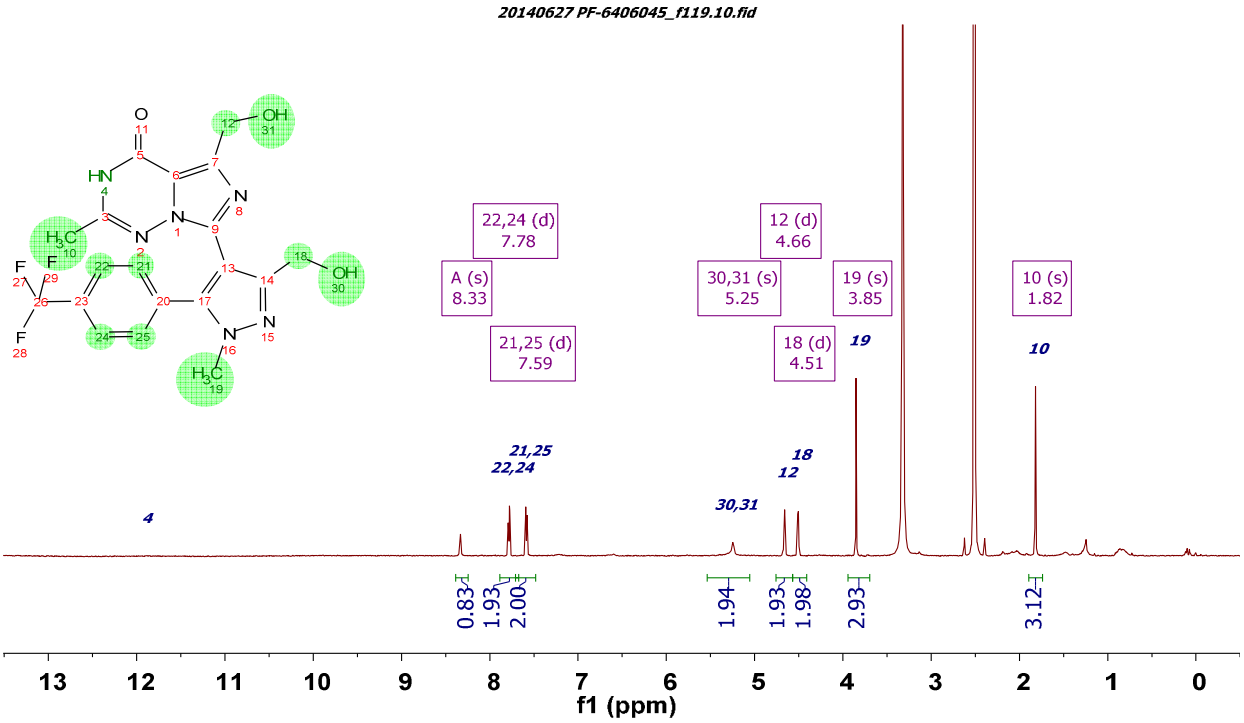

NMR6 The ^{1}H-^{1}H COSY of Compound **1** Fraction 119 (**6**).

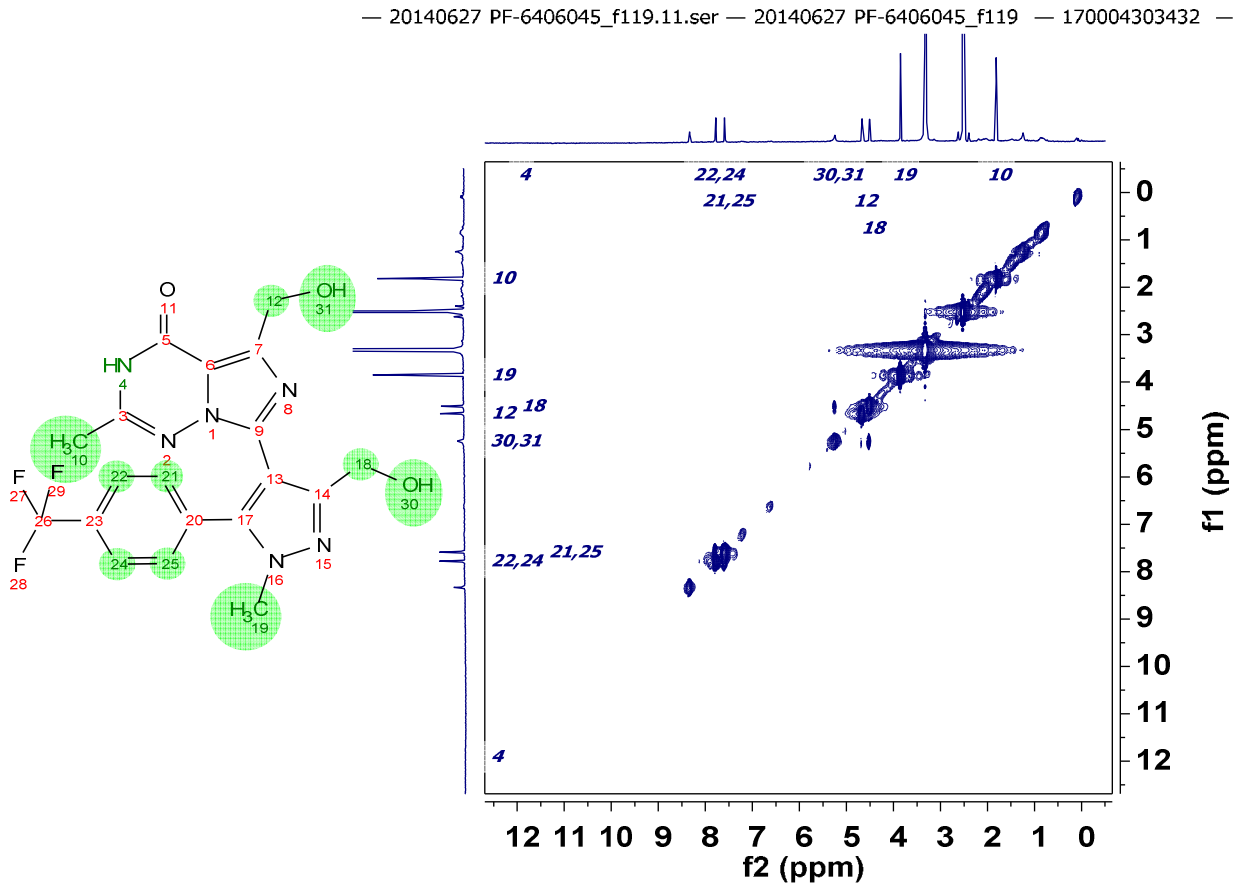

NMR7 The ^{1}H-^{13}C multiplicity edited HSQC of Compound **1** Fraction 119 (**6**).

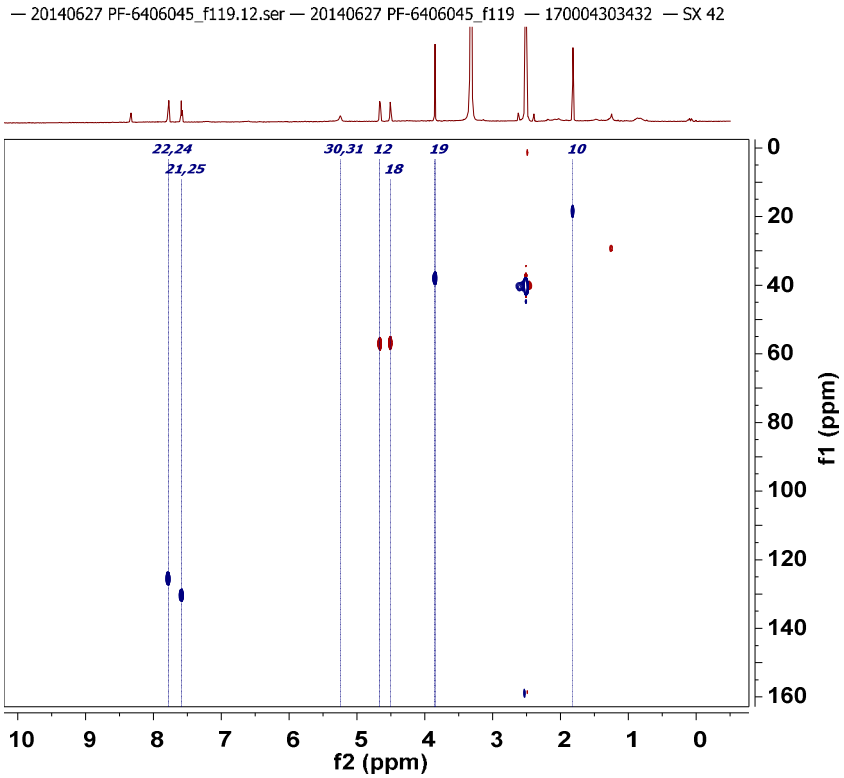

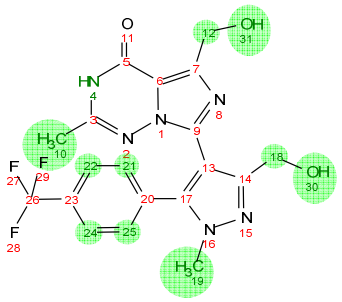

NMR8 The ^{1}H-^{13}C HMBC of Compound **1** Fraction 119 (**6**).

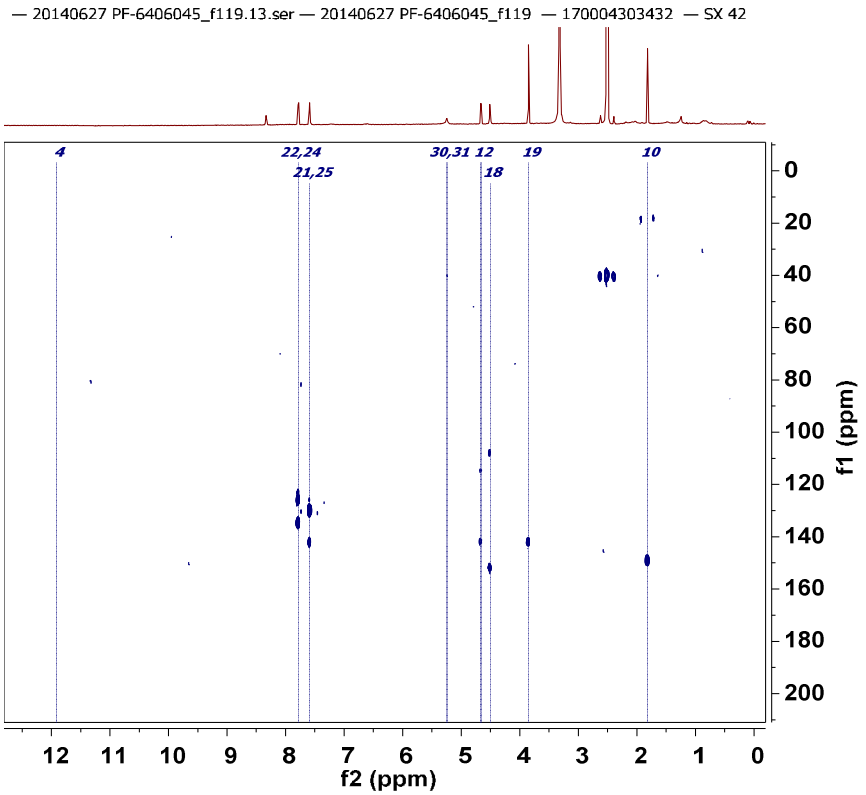

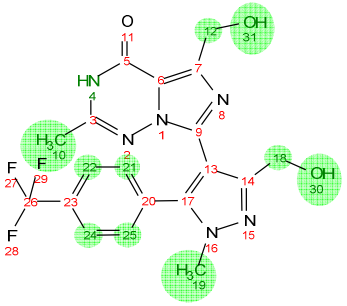

NMR9 The ^{1}H NMR of Compound **1** Fraction 129 (**5**).

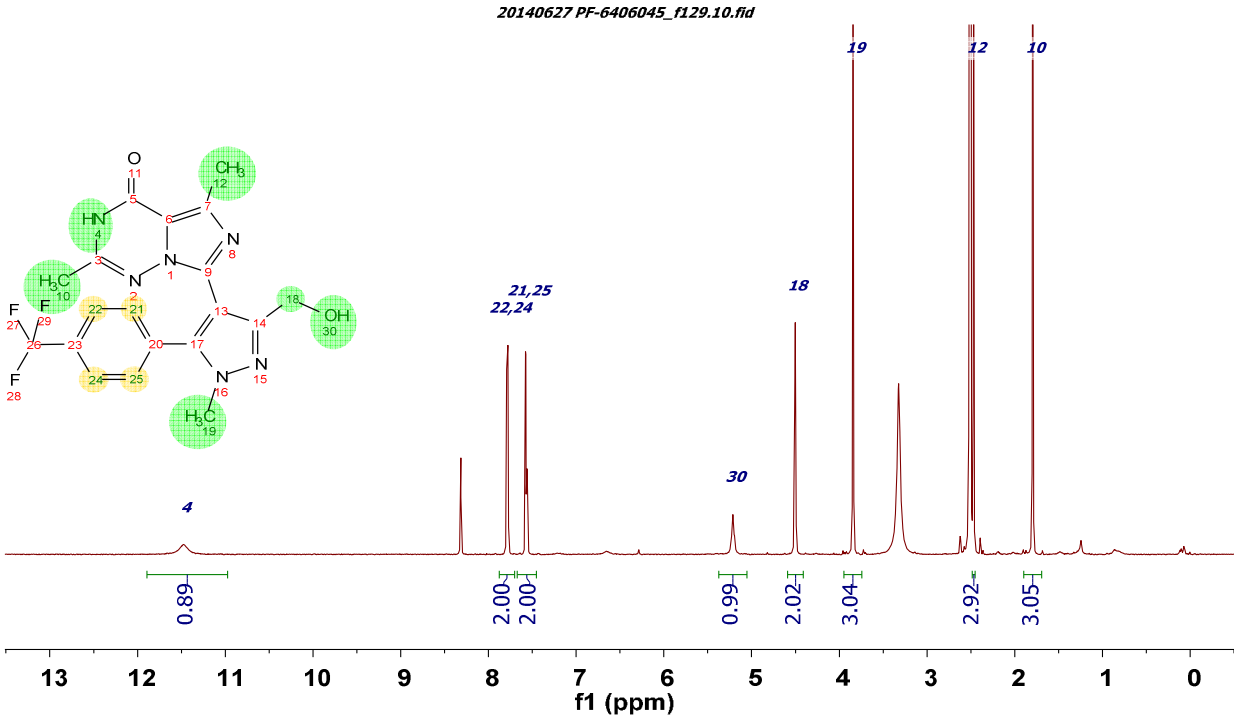

NMR10 The ^{1}H-^{1}H COSY of Compound **1** Fraction 129 (**5**).

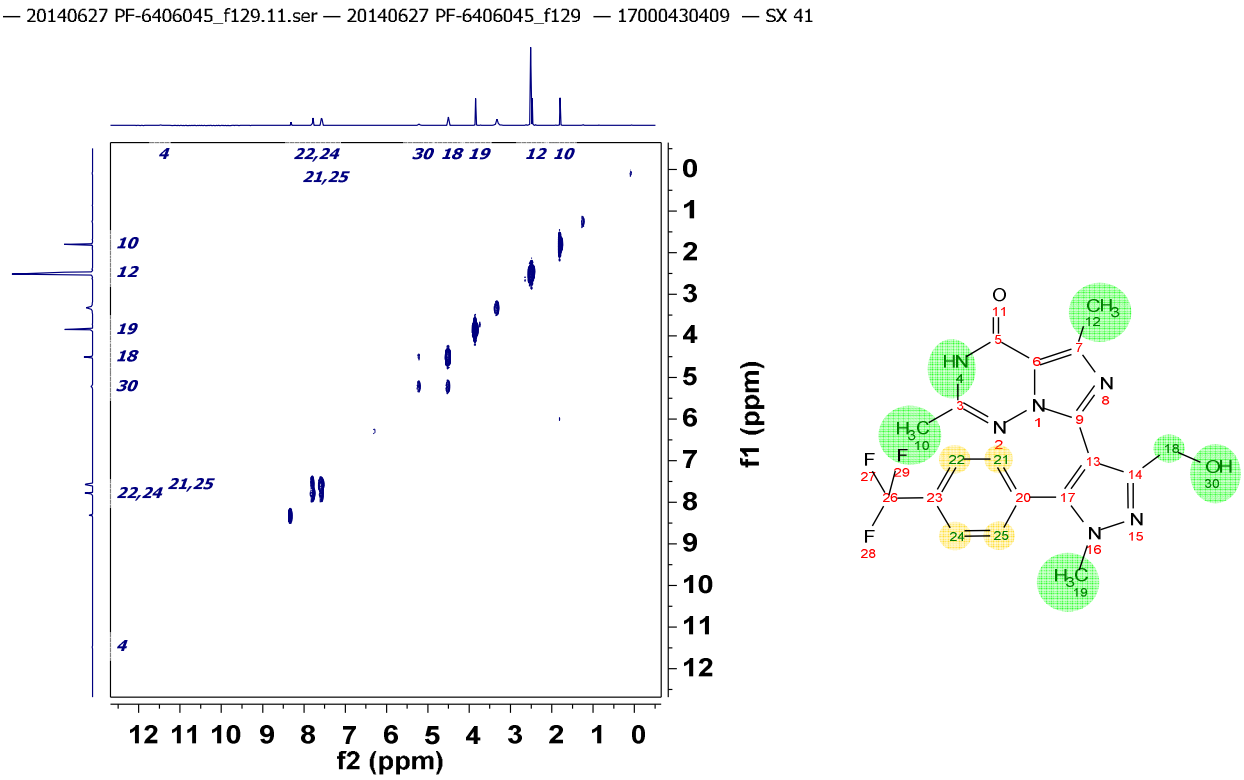

NMR11 The ^{1}H-^{13}C multiplicity edited HSQC of Compound **1** Fraction 129 (**5**).

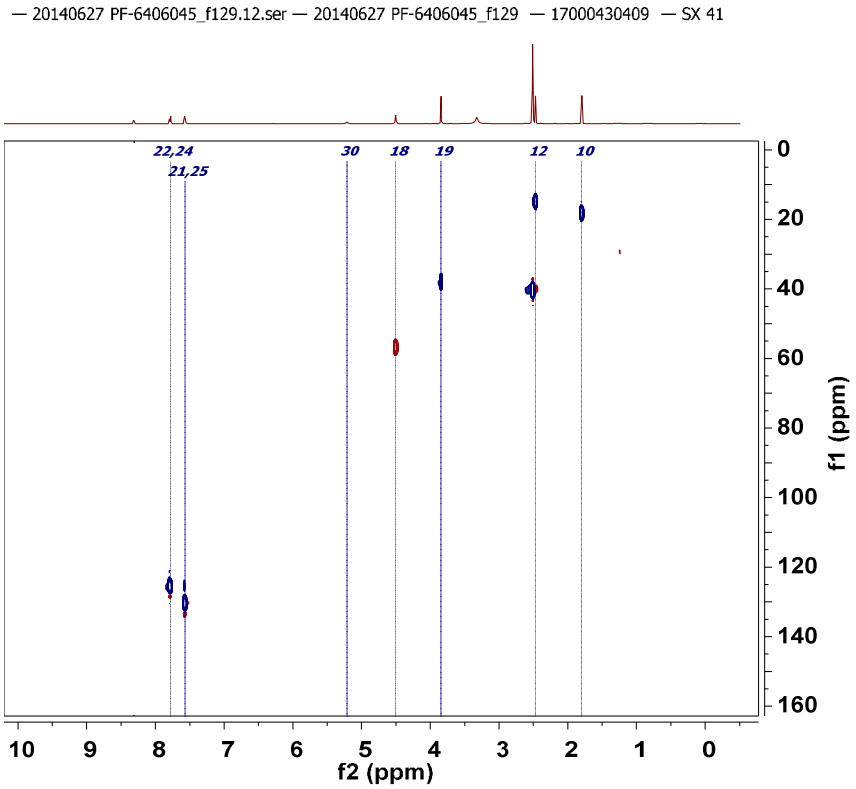

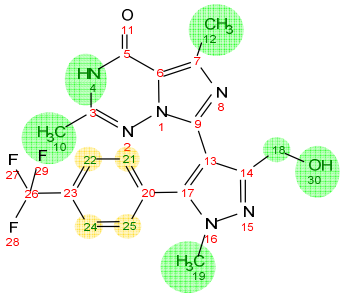

NMR12 The ^{1}H-^{13}C HMBC of Compound **1** Fraction 129 (**5**).

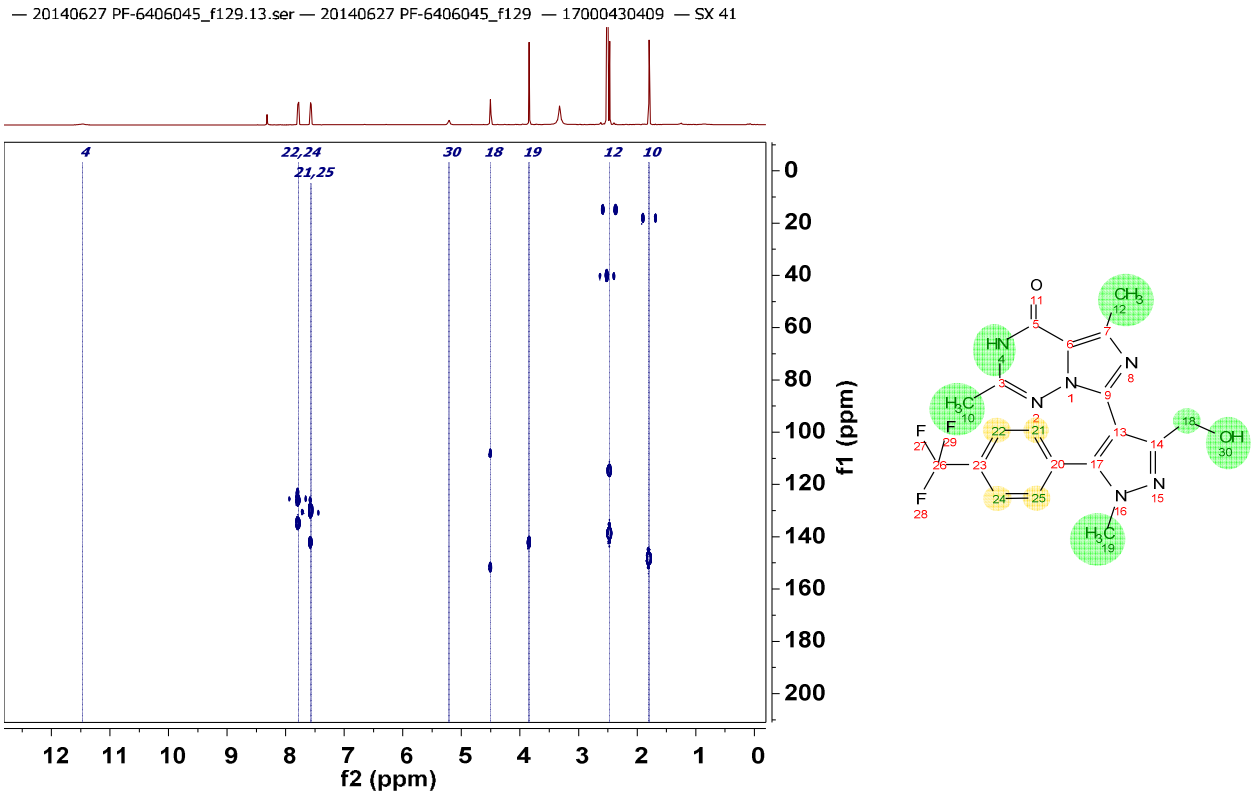

Procedures for Synthesis of 1 and biocatalytic oxidation to 2 (as shown in Scheme 3)

7-Bromo-2,5-dimethylimidazo[5,1-*f*][1,2,4]triazin-4(3*H*)-one (8). To a stirred suspension of the imidazotriazinone **7** (1.25 g, 7.61 mmol) in DMF (15 mL) at 0 °C was added bromine (2.44 g, 15.27 mmol). After 15 min, the ice bath was removed and the reaction mixture was stirred at room temperature. After 3 h, a saturated aqueous solution of $NaHCO_3$ (20 mL) was added and the resulting precipitate was filtered and washed with H_2O. The solid was taken in ether, stirred rigorously, filtered, and dried *in vacuo* to afford bromide **8** as an off-white solid (1.22 g, 65%). ^{1}H NMR (400 MHz, DMSO-d_6): δ 11.78 (br s, 1H), 2.45 (s, 3H), 2.22 (s, 3H). Mass calculated for $[M + H]^+$ ($C_7H_8BrN_4O$) is *m/z* = 243 (100%), 245 (97%), found LCMS $[M+H]^+$ *m/z* = 243, 245.

7-Bromo-2,5-dimethyl-4-(pyrrolidin-1-yl)imidazo[5,1-*f*][1,2,4]triazine (9). To a suspension of compound **8** (1.09 g, 4.48 mmol) in toluene (15 mL) was added phosphorus oxychloride (1.03 mL, 11.20 mmol). Diisopropyl ethylamine (3.99 mL, 22.4 mmol) was added dropwise over 10 min. The reaction mixture was heated to reflux for 3 h, cooled to room temperature, and then concentrated *in vacuo*. The resulting residue was taken up in CH_2Cl_2 (15 mL), cooled to 0 °C, then pyrrolidine (0.74 mL, 9.00 mmol) was added, followed by triethylamine (3.13 mL, 22.4 mmol). The reaction mixture was gradually warmed to room temperature as the ice bath expired. After stirring at room temperature overnight, the reaction mixture was taken up with CH_2Cl_2, and washed with a saturated aqueous solution of $NaHCO_3$ and H_2O. The organic layer was dried over

$MgSO_4$, filtered and filtrate concentrated *in vacuo*. The resulting residue was triturated from diethyl ether and heptane mixture to give triazine **9** as a light brown solid (1.02 g, 77%). ^{1}H NMR (400 MHz, $CDCl_3$): δ 3.84–3.88 (m, 4H), 2.73 (s, 3H), 2.44 (s, 3H), 2.06–2.09 (m, 4H). Mass calculated for $[M + H]^+$ ($C_{11}H_{15}BrN_5$) is *m/z* = 296 (100%), 298 (97%), found LCMS $[M+H]^+$ *m/z* = 296, 298.

Synthesis of boronate ester 10

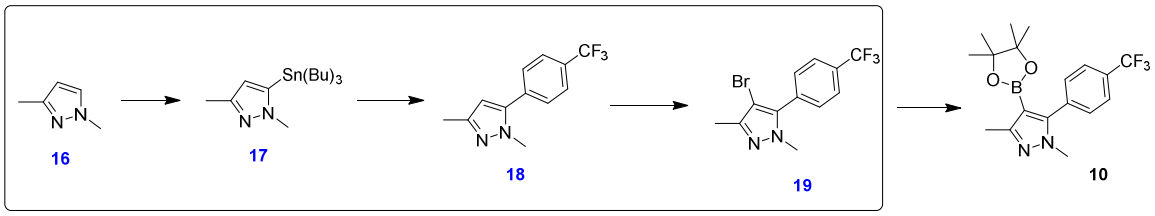

1,3-Dimethyl-5-(tributylstannyl)-1H-pyrazole (17). To a stirred mixture of lithium diisopropylamide (2.0 M in THF, 50 mL, 100 mmol) and *N,N,N',N'*-tetramethyl ethylenediamine (8.36 g, 72.0 mmol) in THF (50 mL) at –65 °C was added 1,3-dimethylpyrazole **16** (8.00 g, 72.0 mmol). After 1 h, tributyltin chloride (30.5 g, 93.6 mmol) was added dropwise over 20 min. The reaction mixture was warmed to –10 °C. After 1 h at –10 °C, a saturated aqueous NH_4Cl solution was added, then extracted four times with EtOAc (100 mL). The organic layers were combined and dried over $MgSO_4$, filtered and filtrate concentrated *in vacuo*. Purification via flash column chromatography on silica gel eluding with 0% to 5% EtOAc in petroleum ether gave stannane **17** as a yellow oil (6.0 g, 22%). ^{1}H NMR (400 MHz, $CDCl_3$): δ 6.04 (s, 1H), 3.85 (s, 3H), 2.28 (s, 3H), 1.51–1.55 (m, 6H), 1.32–1.36 (m, 6H), 1.10–1.13 (m, 6H), 0.88–0.92 (m, 9H). Mass calculated for $[M + H]^+$ ($C_{17}H_{35}N_2Sn$) is *m/z* = 387, found LCMS $[M+H]^+$ *m/z* = 387.

1,3-Dimethyl-5-(4-(trifluoromethyl)phenyl)-1*H*-pyrazole (18). To a degassed solution of the stannane **17** (4.50 g, 11.68 mmol) in DMSO (40 mL) were added 4-bromobenzotrifluoride (5.26 g, 23.4 mmol) and $Pd(PPh_3)_4$ (675 mg, 0.58 mmol). The reaction mixture was evacuated *in vacuo* and filled with N_2, repeated twice more, and then heated to 90 °C under N_2 atmosphere. After 16 h, the reaction mixture was cooled to room temperature, taken up in H_2O, and extracted with EtOAc three times. The combined organic layer was dried over $MgSO_4$, filtered and concentrated *in vacuo*. The resulting residue was purified via flash column chromatography on silica gel eluding with 0% to 10% EtOAc in petroleum ether to afford **18** as a white solid (2.50 g, 89%). ^{1}H NMR (400 MHz, $CDCl_3$): δ 7.70 (d, *J* = 8.4 Hz, 2H), 7.52 (d, *J* = 8.0 Hz, 2H), 6.15 (s, 1H), 2.94 (s, 3H), 2.31 (s. 3H). Mass calculated for $[M + H]^+$ ($C_{12}H_{12}F_3N_2$) is *m/z* = 241, found LCMS $[M+H]^+$ *m/z* = 241.

4-Bromo-1,3-dimethyl-5-(4-(trifluoromethyl)phenyl)-1*H*-pyrazole (19). To a solution of pyrazole **18** (3.00g, 12.5 mmol) in CH_2Cl_2 (50 mL) was added *N*-bromosuccinimide (2.67 g, 15.0 mmol) portionwise. After 3 h, the reaction mixture was concentrated *in*

vacuo and the resulting material was purified via flash column chromatography on silica gel eluding with 0% to 10% EtOAc in petroleum ether to give bromide **19** as a yellow solid (4.50 g, 96%). ^{1}H NMR (400 MHz, $CDCl_3$): δ 7.76 (d, J = 8.0 Hz, 2H), 7.54 (d, J = 8.4 Hz, 2H), 3.77 (s, 3H), 2.29 (s, 3H). Mass calculated for $[M + H]^+$ ($C_{12}H_{11}BrF_3N_2$) is m/z = 319 (100%), 321 (97%), found LCMS $[M+H]^+$ m/z = 319, 321.

1,3-Dimethyl-4-(4,4,5,5-tetramethyl-1,3,2-dioxaborolan-2-yl)-5-(4-(trifluoromethyl)phenyl)-1H-pyrazole (10). To a degassed solution of bromide **19** (4.00g, 12.53 mmol) in dioxane (50 mL) were added 4,4,5,5-tetramethyl-1,3,2-dioxaborolane (6.42 g, 50.1 mmol), triethylamine (6.98 mL, 50.1 mmol), $Pd_2(dba)_3$ (574 mg, 0.63 mmol), and X-Phos (598 mg, 1.25 mmol). The reaction mixture was evacuated *in vacuo* and filled with N_2, repeated twice more, and then heated to 100 °C under N_2 atmosphere. After 16 h, the reaction mixture was cooled to room temperature, filtered through celite, rinsed with EtOAc, and the combined filtrate was concentrated *in vacuo*. The resulting residue was purified via flash column chromatography on silica gel eluding with 10% to 20% EtOAc in petroleum ether to afford compound **10** as an off-white solid (4.00g, 78%). ^{1}H NMR (400 MHz, $CDCl_3$): δ 7.67 (d, J = 8.0 Hz, 2H), 7.50 (d, J = 8.4 Hz, 2H), 3.71 (s, 3H), 2.42 (s, 3H), 1.19 (s, 12H). Mass calculated for $[M + H]^+$ ($C_{18}H_{23}BF_3N_2O_2$) is m/z = 367, found LCMS $[M+H]^+$ m/z = 367.

7-(1,3-dimethyl-5-(4-(trifluoromethyl)phenyl)-1*H*-pyrazol-4-yl)-2,5-dimethylimidazo[5,1-*f*][1,2,4]triazin-4(3*H*)-one (1). To a degassed solution of bromide **9** (980 mg, 3.31 mmol) in dioxane (10 mL) were added boronate **10** (1.45 g, 3.97 mmol), Na_2CO_3 (1.06 g, 9.93 mmol), and $Pd(dppf)Cl_2.CH_2Cl_2$ (139 mg, 0.17 mmol). The reaction mixture was evacuated *in vacuo*, flushed with N_2, and repeated twice more, then heated to 110 °C under N_2 atmosphere. After 16 h, the reaction mixture was cooled to room temperature, filtered over celite, and rinsed with EtOAc. The combined filtrate was washed with H_2O and brine. The organic layer was dried over $MgSO_4$, filtered and the filtrate was concentrated *in vacuo*. The resulting residue was taken up in THF and 1 M HCl (10 mL each) and heated to reflux. After 16 h, the reaction mixture was cooled to room temperature and concentrated *in vacuo*. The resulting residue was taken up in CH_2Cl_2 and washed with a saturated aqueous solution of $NaHCO_3$ and H_2O. The organic layer was dried over $MgSO_4$, filtered, and the filtrate was concentrated *in vacuo*. Purification via flash column chromatography on silica gel eluding with 0% to 10% MeOH in CH_2Cl_2 afforded triazinone **1** as a white solid (714 mg, 53% over 2 steps). ^{1}H NMR (400 MHz, DMSO-d_6): δ 11.45 (s, 1H), 7.76 (d, J = 8 Hz, 2H), 7.54 (d, J = 8 Hz, 2H), 3.80 (s, 3H), 2.45 (s, 3H), 2.20 (s, 3H), 1.87 (s, 3H). ^{13}C NMR (100 MHz, DMSO-d_6): δ 155.6, 148.3, 147.3, 141.9, 138.9, 136.1, 134.5, 130.5, 129.1 (q, J = 21 Hz), 125.6, 124.5 (q, J = 181 Hz), 114.5, 108.4, 37.8, 18.1, 14.8, 12.9. Mass calculated for $[M + H]^+$ ($C_{19}H_{18}F_3N_6O$) is m/z = 403, found LCMS $[M+H]^+$ m/z = 403. Melting point: 227.1–228.4 °C.

Biocatalytic Oxidation of Compound 1 to Compound 2. Iowa medium was prepared (20 g dextrose, 5 g yeast extract, 5 g nutrisoy fluor, 5 g NaCl, 5 g K_2HPO_4, 1 mL P2000,

1 L H_2O) and adjusted to pH 7 with 1 M HCl, then autoclaved to 121 °C for 25 min to sterilize.

Five portions of the following sample were prepared: Saccharothrix aerocolonigenes ATCC 39243 frozen vegetative stock (0.5 mL) was inoculated in sterile Iowa medium (50 mL) in a sterile Nalgene flask and incubated at 30 °C, 210 rpm, 2 inch orbit, for 2 d. The content was then inoculated into sterile Iowa medium (500 mL) and incubated as above. After 2 d, a solution of compound **1**(102 mg, 0.25 mmol) in DMSO (20 mL) was added and incubated at 30 °C. After 7 d, the whole broth was extracted twice with an equal volume of methyl ethylketone. The organic phases were combined, dried over $MgSO_4$, filtered and concentrated *in vacuo*. The resulting oil was purified via SFC on 2EP column with 15-50% MeOH and lyophilized to afford product **2** as a white powder (101 mg total, 20%).

Procedures for Synthesis of Compound 2 (as shown in Scheme 4)

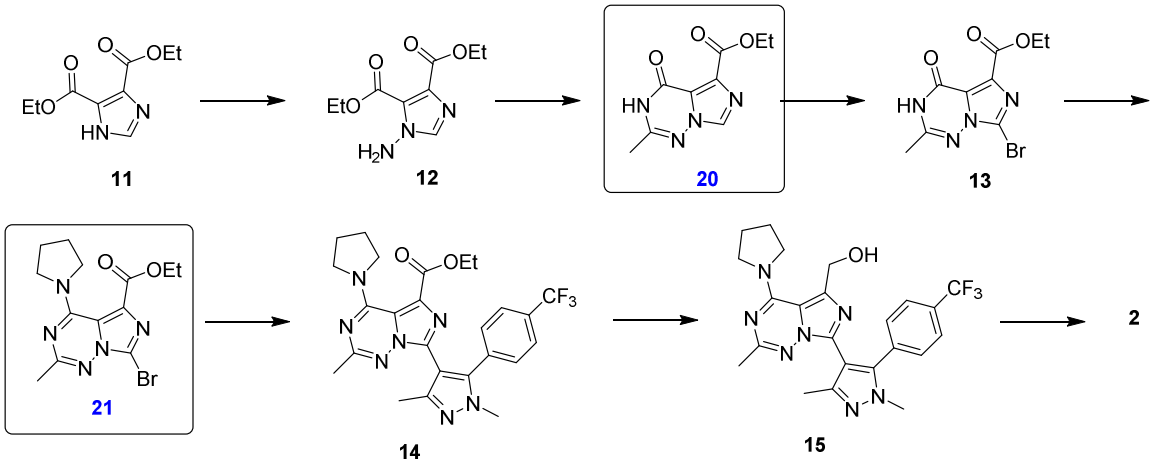

Diethyl 1-amino-1*H*-imidazole-4,5-dicarboxylate (12). To a suspension of imidazole **11** (2.50 g, 11.8 mmol) in H_2O (25 mL) and EtOH (5 mL) at 0 °C was added K_2CO_3 (8.22 g, 58.9 mmol). After 15 min, hydroxylamine-*O*-sulfonic acid (4.00 g, 35.3 mmol) was added portionwise. The reaction mixture was gradually warmed to room temperature as the ice bath expired. After 20 h, the reaction mixture was filtered, washed with CH_2Cl_2, the filtrate was poured into a separatory funnel and extracted three times with CH_2Cl_2. The organic layers were combined, dried over MgSO4, filtered and the filtrate was concentrated *in vacuo* to afford amino-imidazole **12** as a clear yellow oil (2.08 g, 78%). ^{1}H NMR (400 MHz, DMSO-d_6): δ 7.76 (s, 1H), 6.31 (s, 2H), 4.30 (q, J = 8 Hz, 2H), 4.21 (q, J = 8 Hz, 2H), 1.29 (t, J = 8 Hz, 3H), 1.24 (t, J = 8 Hz, 3H). ^{13}C NMR (100 MHz, DMSO-d_6): δ 162.3, 160.1, 139.9, 131.9, 127.7, 61.8, 60.8, 14.5, 14.3. Mass calculated for $[M + H]^+$ ($C_9H_{14}N_3O_4$) is m/z = 228.0979, found HRMS (ESI) $[M+H]^+$ m/z = 228.0974.

2,5-Dimethylimidazo[5,1-*f*][1,2,4]triazin-4(3*H*)-one (20). To a suspension of the imidazole **12** (1.14 g, 5.02 mmol) in 2-Me-THF (15 mL) were added ethyl acetimidate hydrochloride (2.17 g, 17.6 mmol) and diisopropyl ethylamine (4.46 mL, 25.1 mmol) and the mixture was heated to reflux. After 16 h, the reaction mixture was cooled to room

temperature and concentrated *in vacuo*. Trituration from EtOAc and EtOH mixture afforded triazinone **20** as a white solid (602 mg, 54%). ^{1}H NMR (400 MHz, DMSO-d_6): δ 12.09 (br s, 1H), 8.64 (s, 1H), 4.29 (q, J = 7.2 Hz, 2H), 2.24 (s, 3H), 1.31(t, J = 7.2 Hz, 3H). ^{13}C NMR (100 MHz, DMSO-d_6): δ 161.7, 152.8, 151.1, 134.3, 130.5, 120.5, 60.9, 18.4, 14.6. Mass calculated for $[M + H]^+$ ($C_9H_{10}N_4O_3$) is m/z = 223.0826, found HRMS (ESI) $[M+H]^+$ m/z = 223.0823.

Ethyl 7-bromo-2-methyl-4-oxo-3,4-dihydroimidazo[5,1-*f*][1,2,4]triazine-5-carboxylate (13). To a solution of the triazione **20** (987 mg, 4.44 mmol) in MeCN (10 mL) and acetic acid (2 mL) was added N-bromosuccinimide (2.47 g, 13.3 mmol). The reaction mixture was heated to 70 °C. After 16 h, the reaction mixture was cooled to room temperature and concentrated *in vacuo*. Trituration from EtOAc and EtOH mixture gave bromide **13** as a white solid (1.17 g, 88%). ^{1}H NMR (400 MHz, DMSO-d_6): δ 12.25 (br s, 1H), 4.29 (q, J = 6.8 Hz, 2H), 2.27 (s, 3H), 1.30 (t, J = 6.8 Hz, 3H). ^{13}C NMR (100 MHz, DMSO-d_6): δ 160.7, 152.3, 151.6, 130.7, 123.3, 118.0, 61.2, 18.7, 14.5. Mass calculated for $[M + H]^+$ ($C_9H_9BrN_4O_3$) is m/z = 300.9931, found HRMS (ESI) $[M+H]^+$ m/z = 300.9928.

Ethyl 7-bromo-2-methyl-4-(pyrrolidin-1-yl)imidazo[5,1-*f*][1,2,4]triazine-5-carboxylate (21). To a suspension of 1,2,4-triazole (22.9 g, 332 mmol) in MeCN (200 mL) at 0 °C was added phosphorus oxychloride (12.2 mL, 133 mmol). A white suspension was observed. Triethylamine (55.5 mL, 399 mmol) was added dropwise over 30 min. After 15 min, the ice bath was removed and the reaction mixture was stirred at room temperature for 30 min, then intermediate **13** (10.0 g, 33.2 mmol) was added portionwise. The reaction mixture was heated to 60 °C for 20 h, cooled to 0 °C, then slowly quenched with a saturated aqueous solution of $NaHCO_3$. The mixture was extracted twice with CH_2Cl_2, the organic layers were combined, dried over $MgSO_4$, filtered, and the filtrate concentrated *in vacuo*. The resulting crude triazole was taken onto next step.

The material from above was taken up in CH_2Cl_2 (200 mL), cooled to 0 °C, then diisopropyl ethylamine (11.1 mL, 62.5 mmol) was added slowly, followed by dropwise addition of pyrrolidine (7.62 mL, 93.7 mmol) over 15 min. The ice bath was removed and the reaction mixture was stirred at room temperature. After 5 h, the reaction mixture was taken up with CH_2Cl_2, and washed with a saturated aqueous solution of $NaHCO_3$ and H_2O. The organic layer was dried over MgSO4, filtered and filtrate concentrated *in vacuo*. Purification via flash column chromatography on silica gel eluding with 0% to 50% EtOAc in heptane furnished triazine **21** as a white solid (10.1 g, 86%). ^{1}H NMR (400 MHz, $CDCl_3$): δ 4.35 (q, J = 7.2 Hz, 2H), 3.70 (t, J = 6.8 Hz, 4H), 2.34 (s, 3H), 1.89 (br s, 4H), 1.36 (t, J = 7.2 Hz, 3H). Mass calculated for $[M + H]^+$ ($C_{13}H_{17}BrN_5O_2$) is m/z = 354 (100%), 356 (97%), found LCMS $[M+H]^+$ m/z = 354, 356.

Ethyl 7-(1,3-dimethyl-5-(4-(trifluoromethyl)phenyl)-1*H*-pyrazol-4-yl)-2-methyl-4-(pyrrolidin-1-yl)imidazo[5,1-*f*][1,2,4]triazine-5-carboxylate (14). To a degassed solution of triazine **21** (10.0 g, 28.2 mmol) in dioxane (150mL) and H_2O (30 mL) were added boronate **10** (11.4 g, 31.1 mmol), Na_2CO_3 (9.07 g, 84.7 mmol) and $Pd(dppf)Cl_2.CH_2Cl_2$ (1.19 g, 1.41 mmol). The reaction mixture was evacuated *in vacuo*

and filled with N_2, repeated twice more, and then heated to 110 °C under N_2 atmosphere. After 16 h, the reaction mixture was cooled to room temperature, filtered over celite, rinsed with EtOAc. The filtrate was taken up with more EtOAc and washed with H_2O and brine. The organic layer was dried over $MgSO_4$, filtered, and the filtrate was concentrated *in vacuo*. The resulting residue was purified via flash column chromatography on silica gel eluding with 40% to 80% EtOAc in heptane to afford intermediate **14** as a beige solid (13.1 g, 91%). ^{1}H NMR (400 MHz, $CDCl_3$): δ 7.58 (d, *J* = 8 Hz, 2H), 7.45 (d, *J* = 8 Hz, 2H), 4.41 (q, *J* = 7.2 Hz, 2H), 3.81 (s, 3H), 3.75 (br s, 4H), 2.33 (s, 3H), 2.09 (s, 3H), 1.93 (br s, 4H), 1.40 (t, *J* = 6.8 Hz, 3H). Mass calculated for $[M + H]^+$ ($C_{25}H_{27}F_3N_7O_2$) is *m/z* = 514, found LCMS $[M+H]^+$ *m/z* = 514.

(7-(1,3-Dimethyl-5-(4-(trifluoromethyl)phenyl)-1*H*-pyrazol-4-yl)-2-methyl-4-(pyrrolidin-1-yl)imidazo[5,1-*f*][1,2,4]triazin-5-yl)methanol (15). To a solution of the ester **14** (6.97 g, 13.6 mmol) in THF (80 mL) was added $LiBH_4$ solution (2 M in THF, 10.2 mL, 20.4 mmol) dropwise over 5 min. The reaction mixture was heated to 50 °C for 16 h, then cooled to 0 °C, then HCl (2N, 30 mL) was added dropwise over 30 min. The mixture was taken up in EtOAc, washed with 1 M NaOH and H_2O. The organic layer was dried over $MgSO_4$, filtered and the filtrate was concentrated *in vacuo* to afford crude alcohol **15** as a beige solid (6.30 g, 98%), which was taken onto next step without further purification. ^{1}H NMR (400 MHz, MeOD): δ 7.76 (d, *J* = 8 Hz, 2H), 7.57 (d, *J* = 8 Hz, 2H), 5.03 (s, 2H), 3.88 (s, 3H), 3.60–3.65 (m, 4H), 2.35 (s, 3H), 2.20 (s, 3H), 2.14 (br s, 4H). Mass calculated for $[M + H]^+$ ($C_{23}H_{25}F_3N_7O$) is *m/z* = 472, found LCMS $[M+H]^+$ *m/z* = 472.

7-(1,3-Dimethyl-5-(4-(trifluoromethyl)phenyl)-1*H*-pyrazol-4-yl)-5-(hydroxymethyl)-2-methylimidazo[5,1-*f*][1,2,4]triazin-4-(3*H*)-one (2). A solution of the triazine **15** (6.30 g, 13.4 mmol) in THF and 1 M HCl (50 mL each) was heated to 75 °C. After 16 h, the reaction mixture was cooled to room temperature and concentrated *in vacuo*. The resulting residue was triturated from a saturated aqueous solution of $NaHCO_3$ and filtered. The resulting solid was purified via flash column chromatography on silica gel eluding with 0% to 5% MeOH in EtOAc to afford the product **2** as a white solid (5.14 g, 92%). ^{1}H NMR (400 MHz, $CDCl_3$): δ 10.1 (br s, 1H), 7.63 (d, *J* = 8 Hz, 2H), 7.42 (d, *J* = 8 Hz, 2H), 4.93 (s, 2H), 4.26 (br s, 1H), 3.84 (s, 3H), 2.36 (s, 3H), 2.05 (s, 3H). ^{13}C NMR (100 MHz, $CDCl_3$): δ 156.9, 148.6, 146.2, 145.6, 142.6, 137.9, 133.9, 130.7 (appar. d, *J* = 33 Hz), 129.9, 125.3, 125.2 (appar. d, *J* = 271 Hz), 113.6, 107.6, 59.8, 37.4, 18.2, 12.8. Mass calculated for $[M + H]^+$ ($C_{19}H_{18}F_3N_6O_2$) is *m/z* = 419, found LCMS $[M+H]^+$ *m/z* = 419. Melting point: 206–209 °C.

1. NMR Spectra:

Compound 8 (^{1}H NMR in DMSO-d_6)

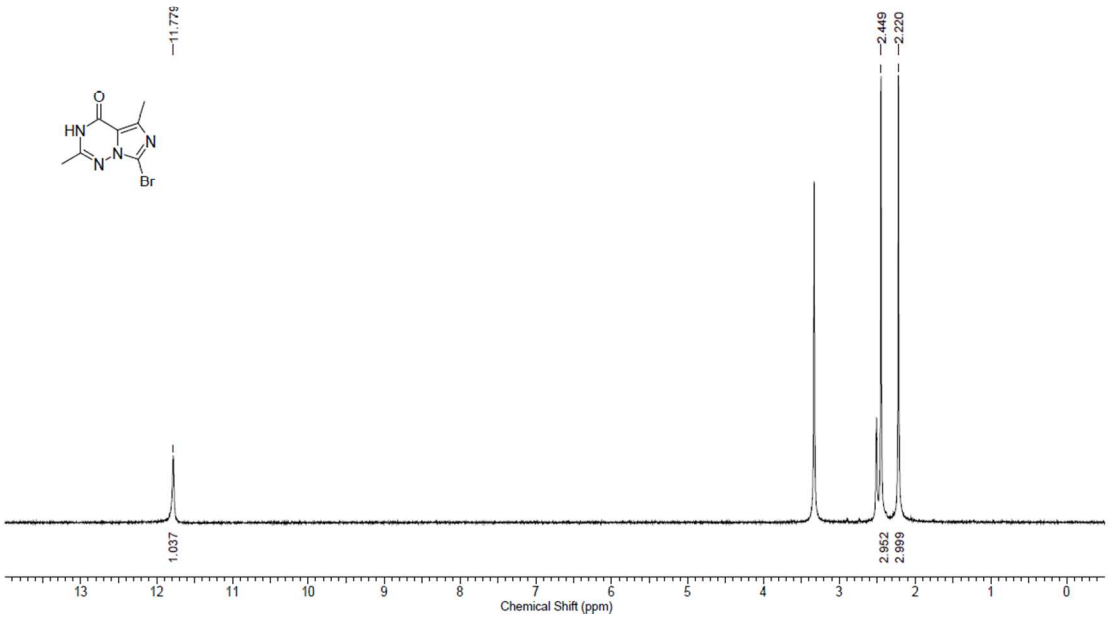

Compound 9 (^{1}H NMR in $CDCl_3$)

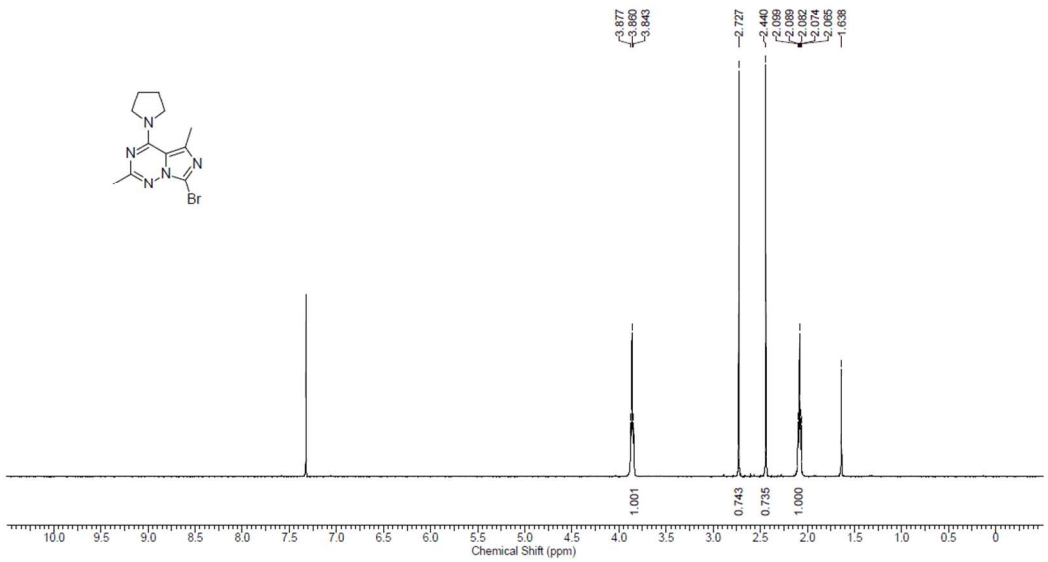

Compound 17 (^{1}H NMR in $CDCl_3$)

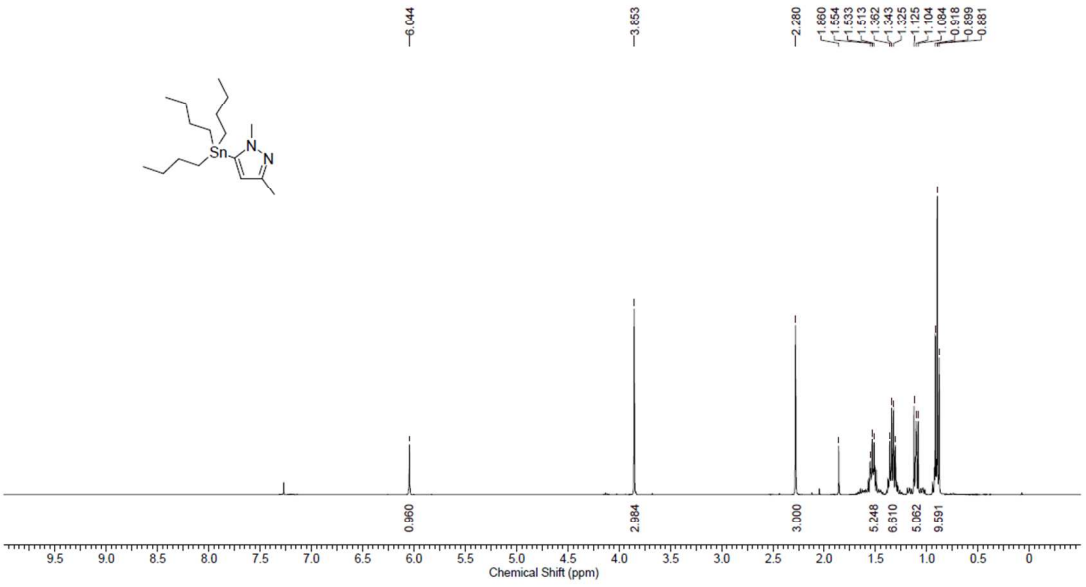

Compound 18 (^{1}H NMR in $CDCl_3$)

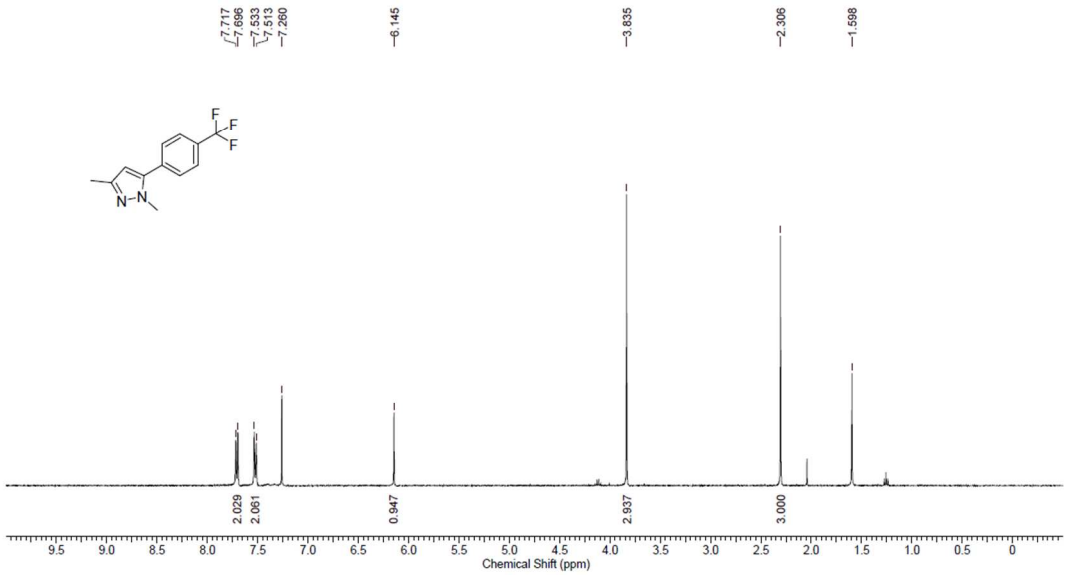

Compound 19 (^{1}H NMR in $CDCl_3$)

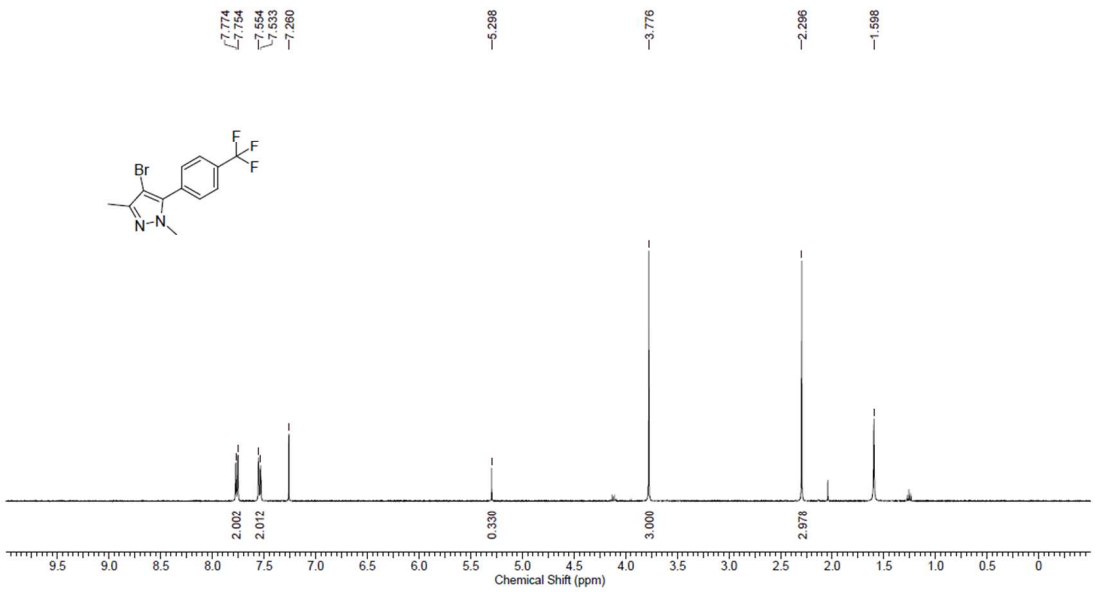

Compound 10 (^{1}H NMR in $CDCl_3$)

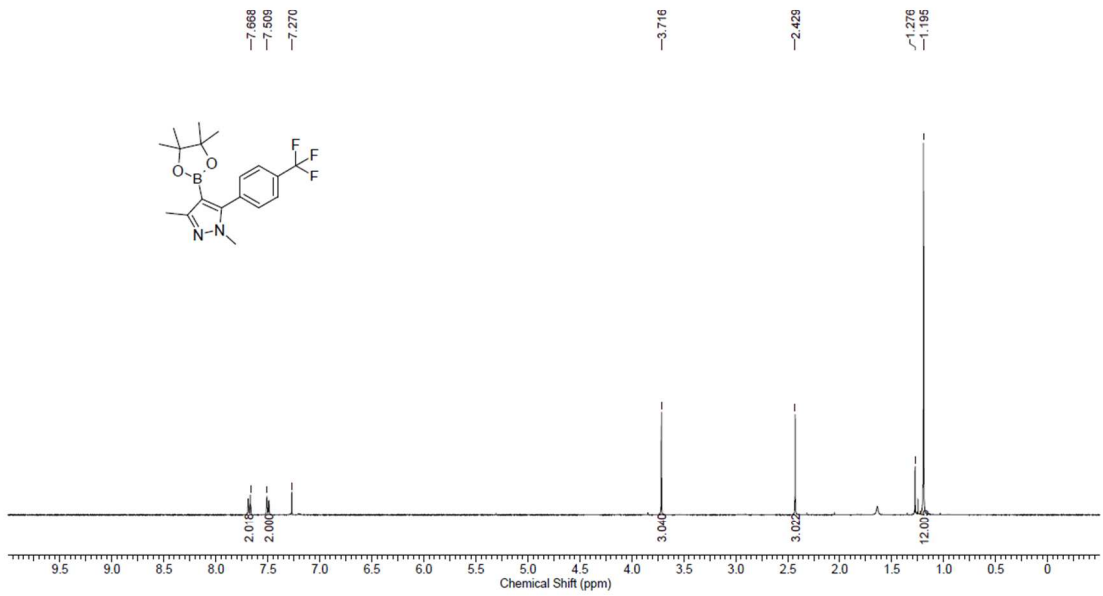

Compound 1 (^{1}H NMR in DMSO-d_6)

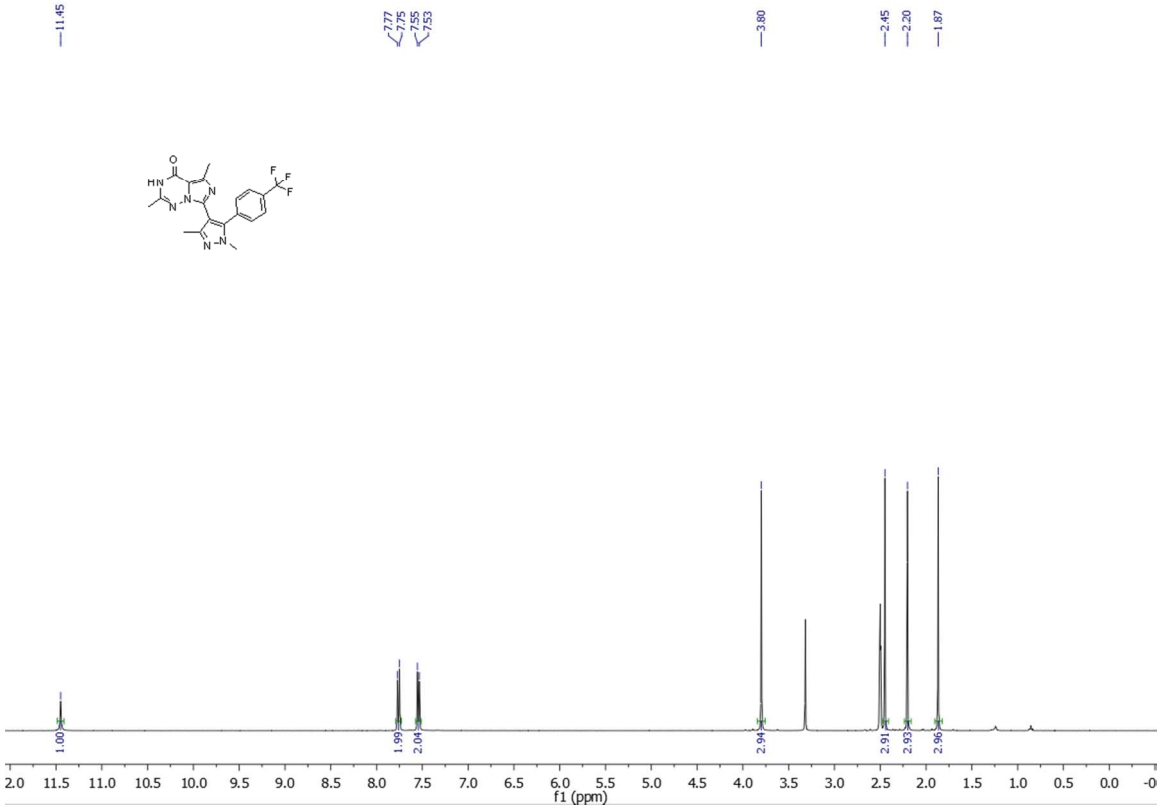

Compound 1 (^{13}C NMR in DMSO-d_6)

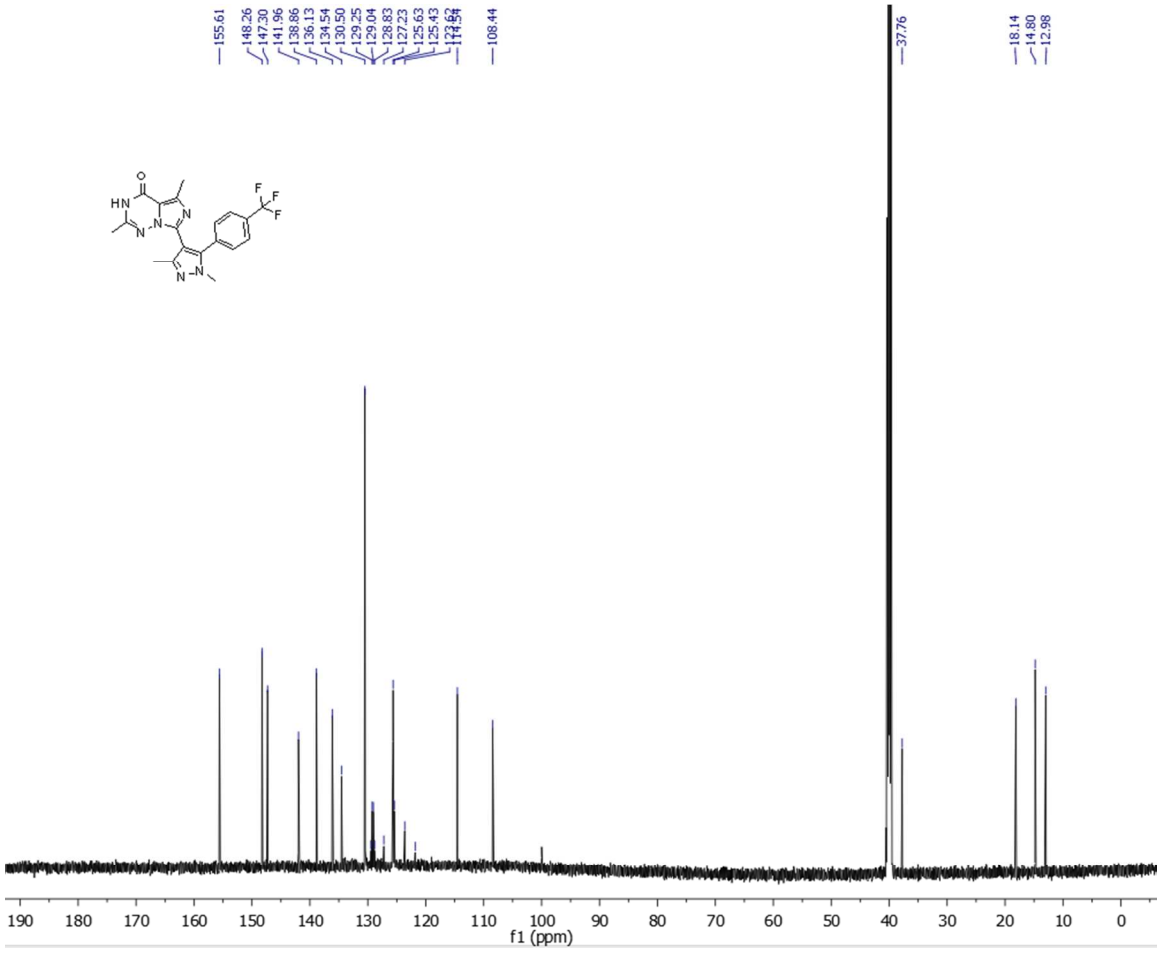

Compound 12 (1H NMR in DMSO-d_6)

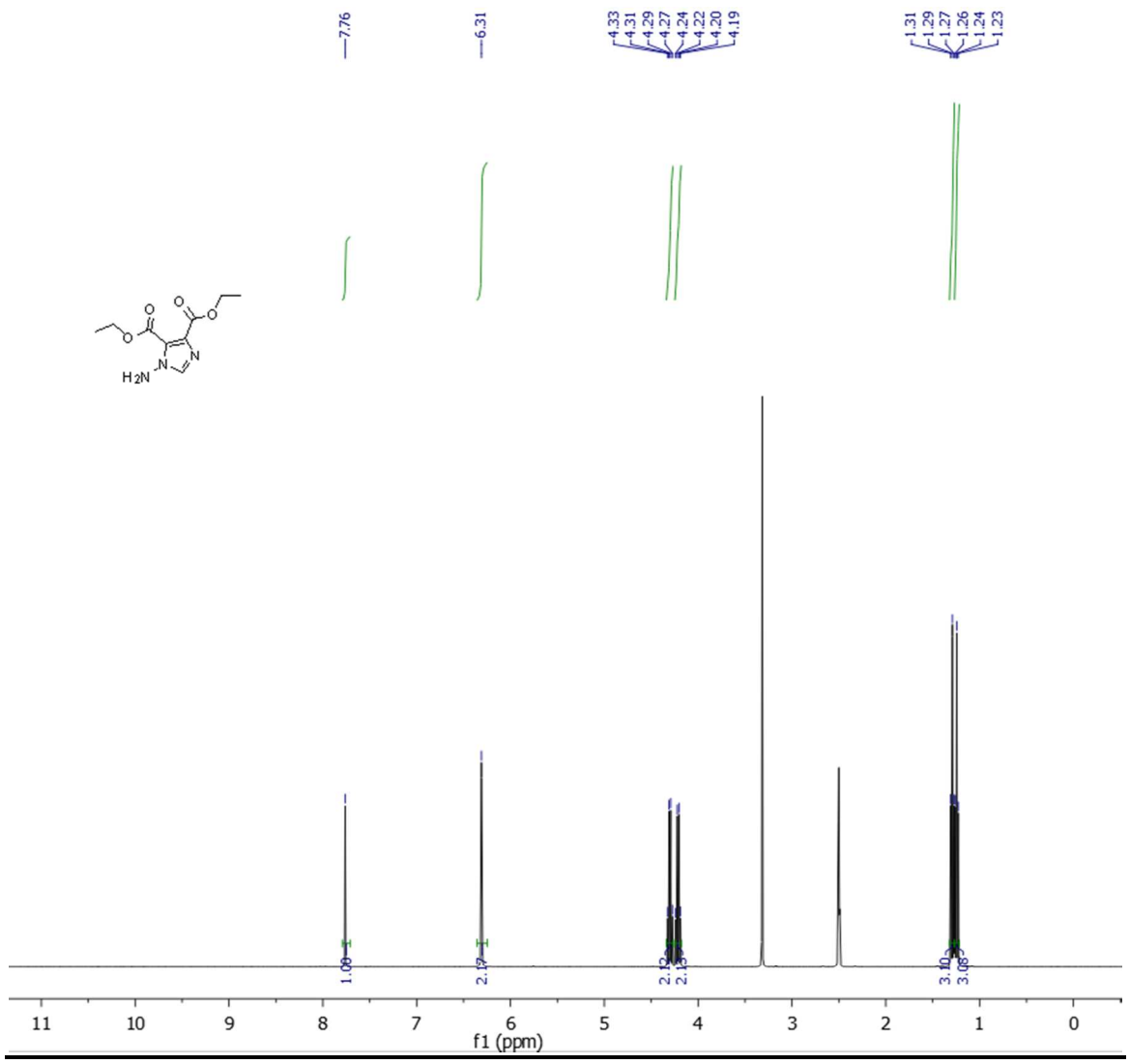

Compound 12 (^{13}C NMR in DMSO-d_6)

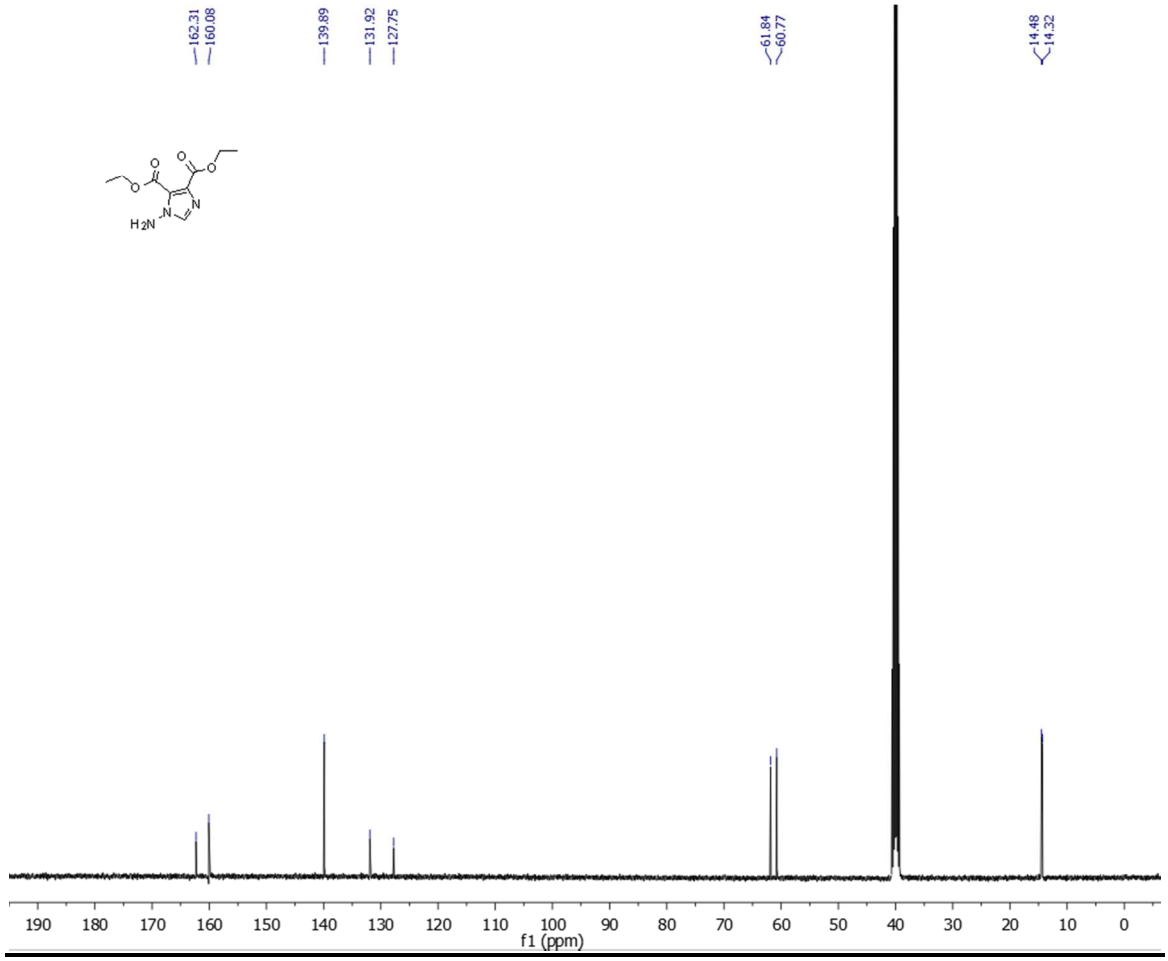

Compound 20 (^{1}H NMR in DMSO-d_6)

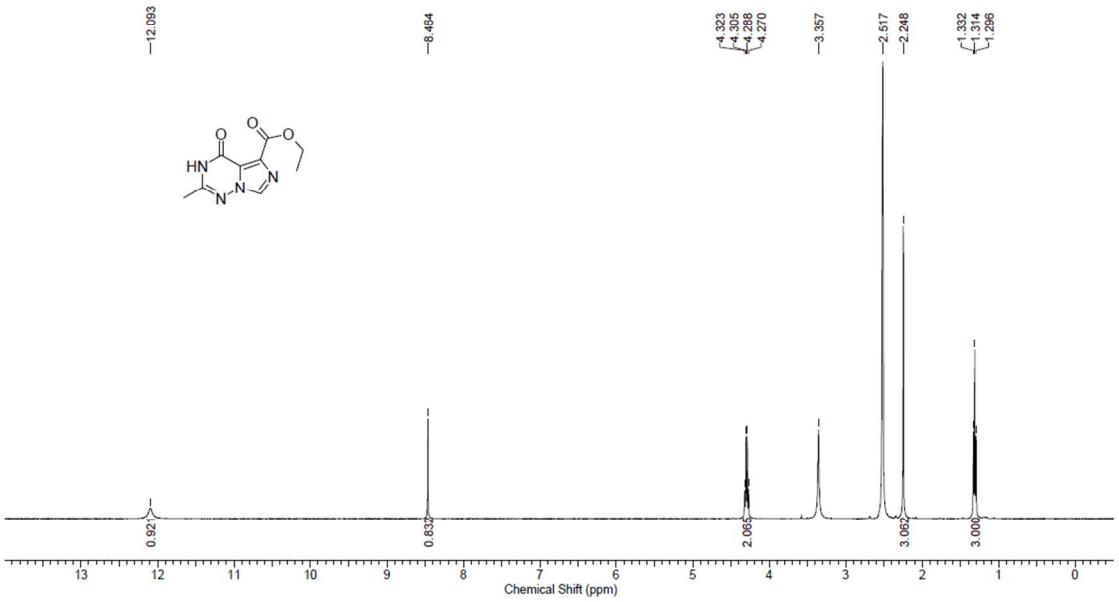

Compound 20 (^{13}C NMR in DMSO-d_6)

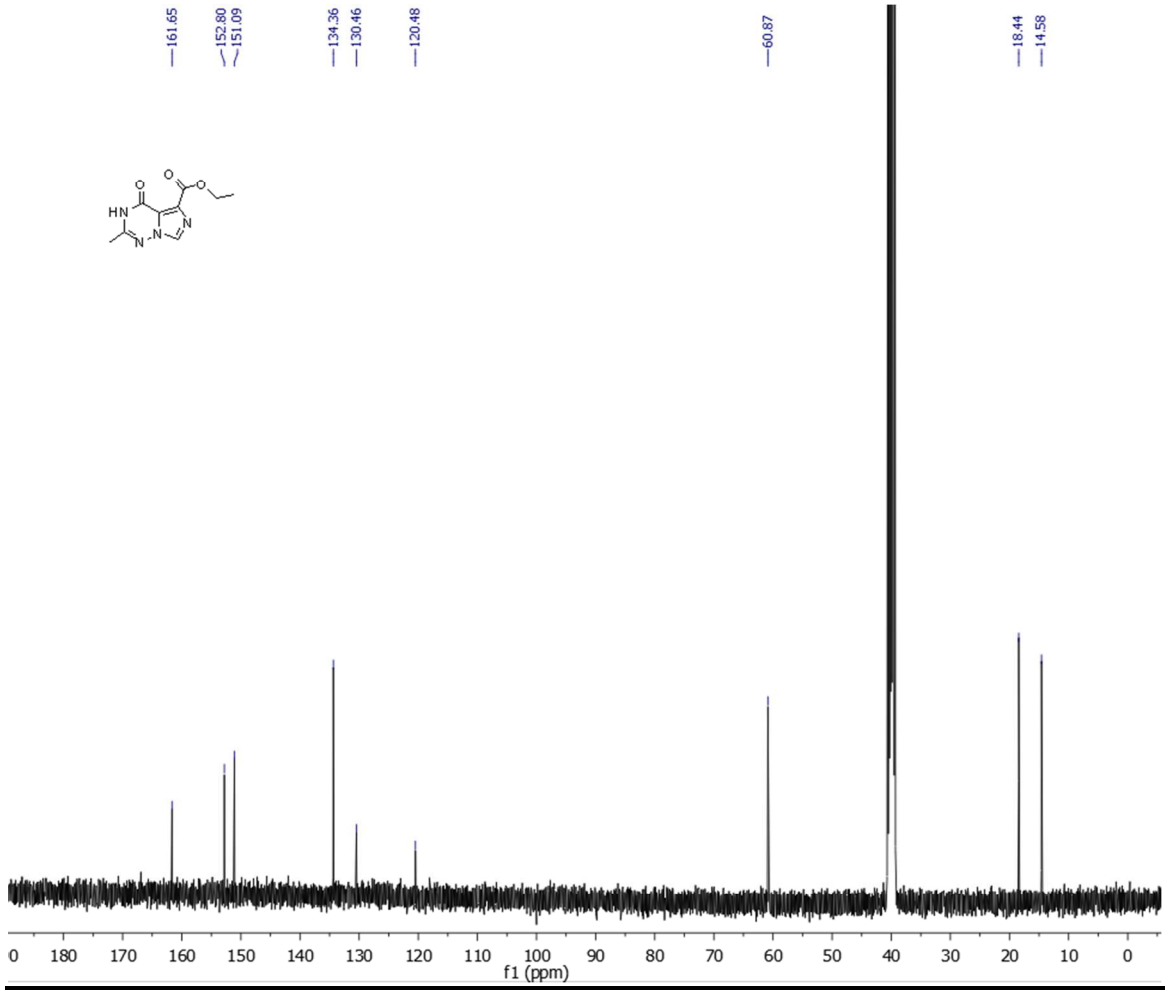

Compound 13 (^{1}H NMR in DMSO-d_6)

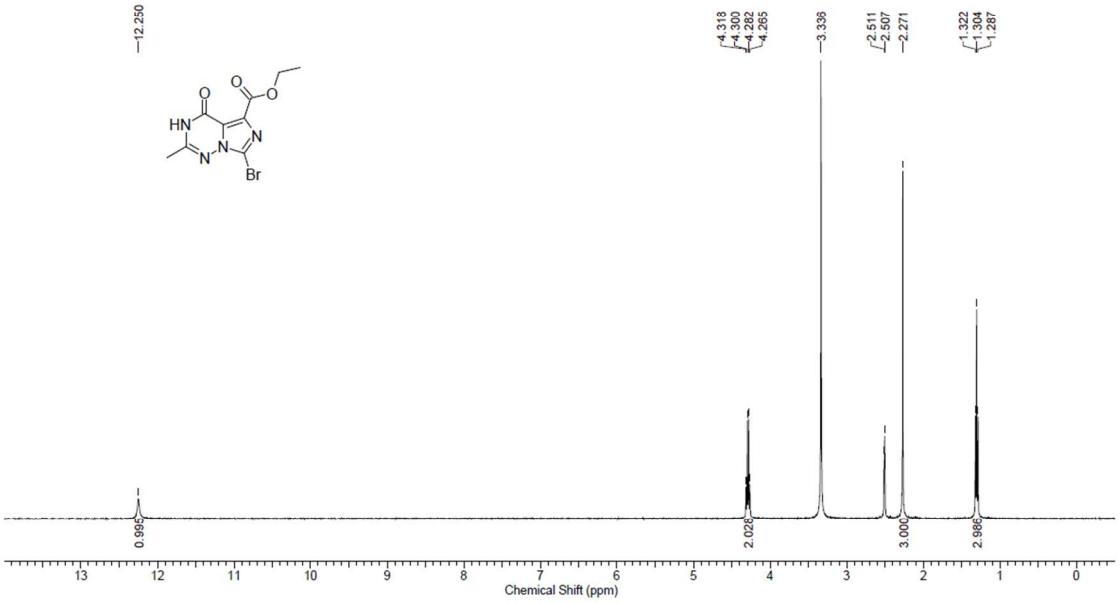

Compound 13 (^{13}C NMR in DMSO-d_6)

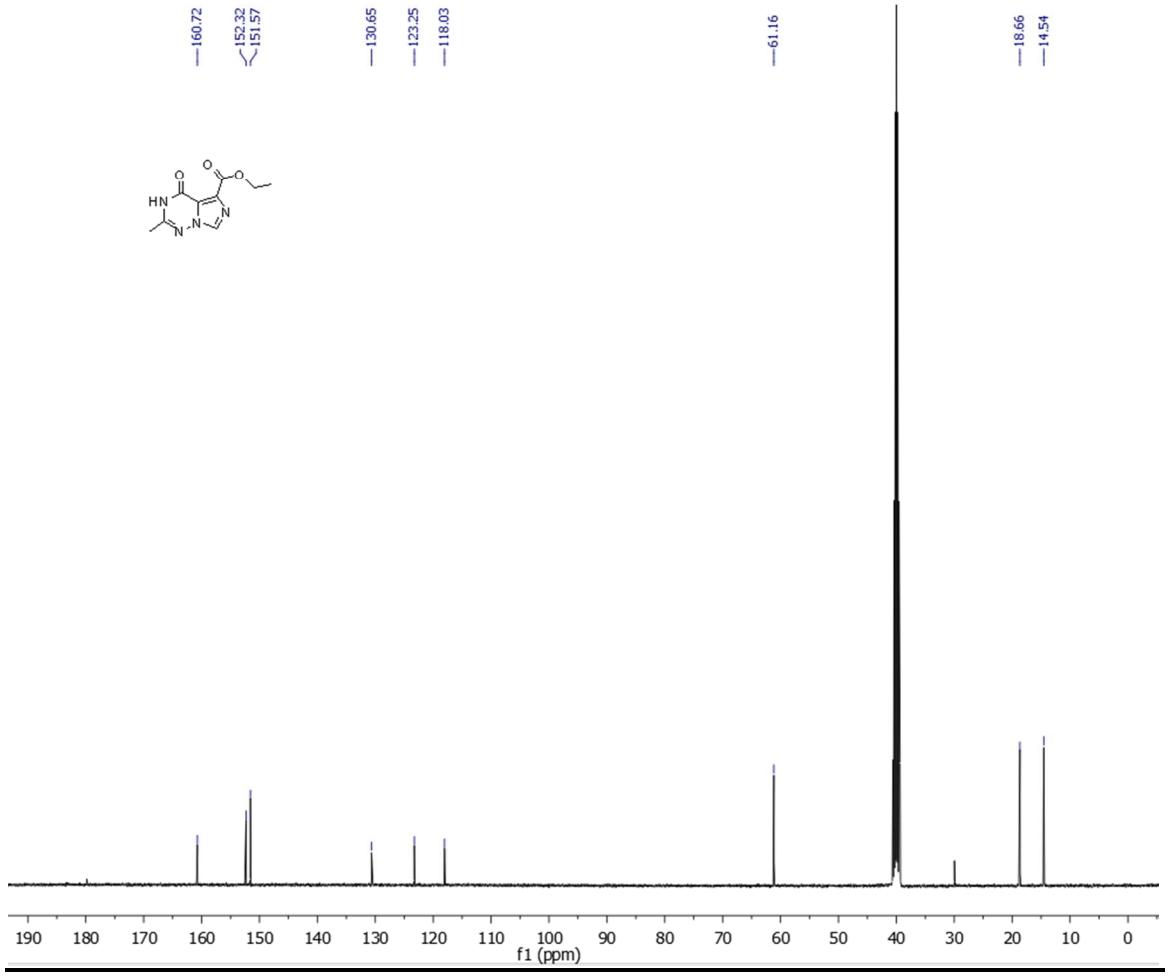

Compound 21 (^{1}H NMR in $CDCl_3$)

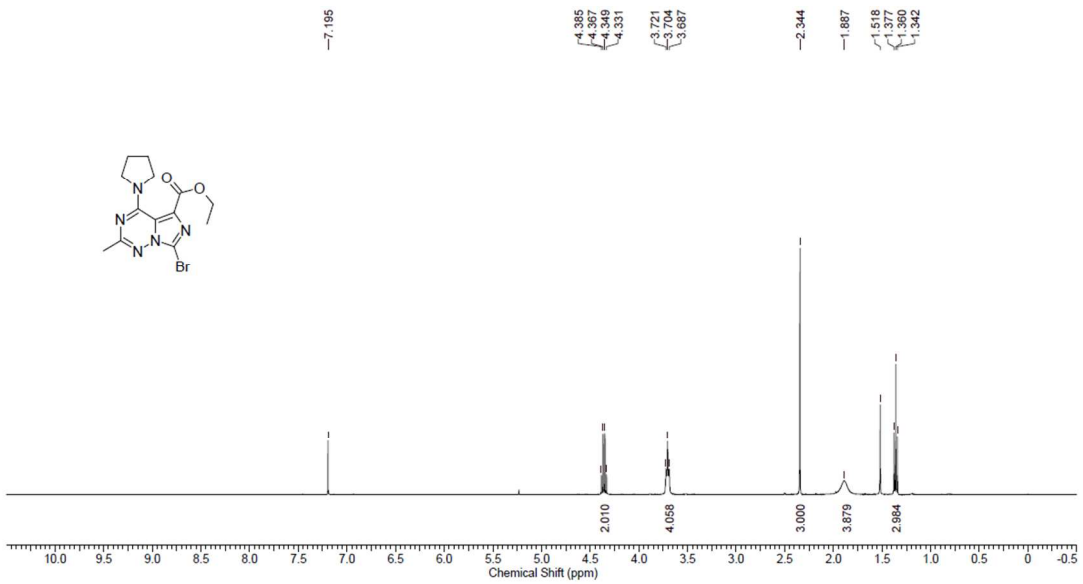

Compound 14 (^{1}H NMR in $CDCl_3$)

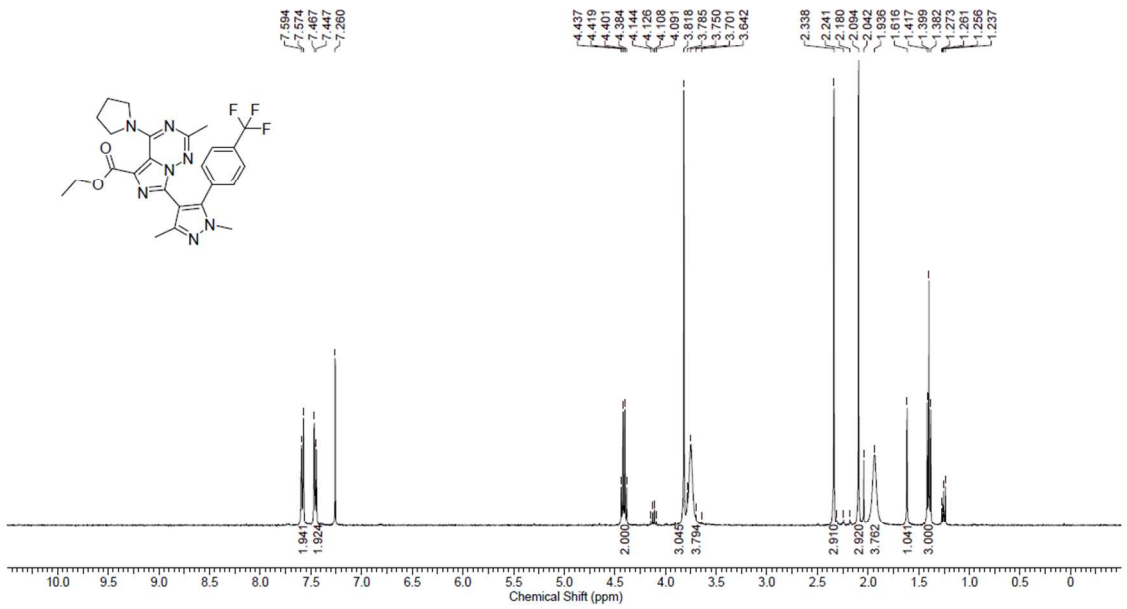

Compound 15 (^{1}H NMR in MeOD)

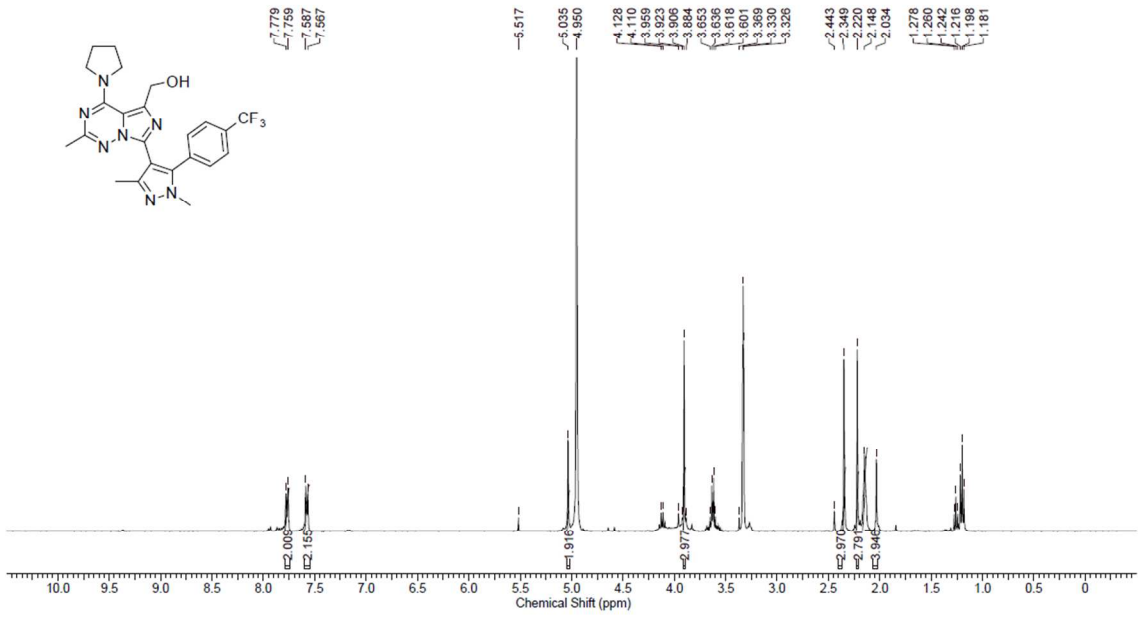

Compound 2 (^{1}H NMR in $CDCl_3$)

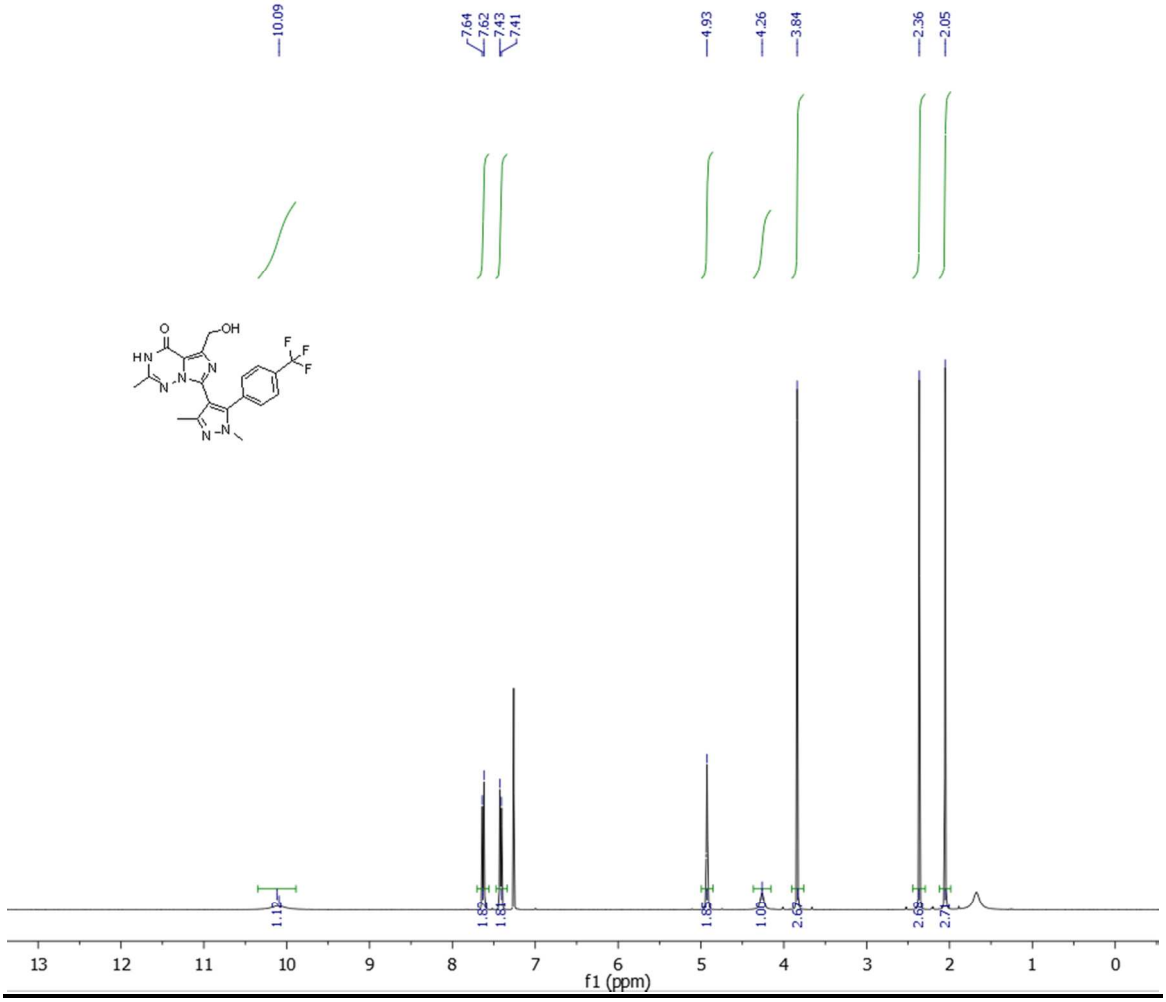

Compound 2 (^{13}C NMR in $CDCl_3$)

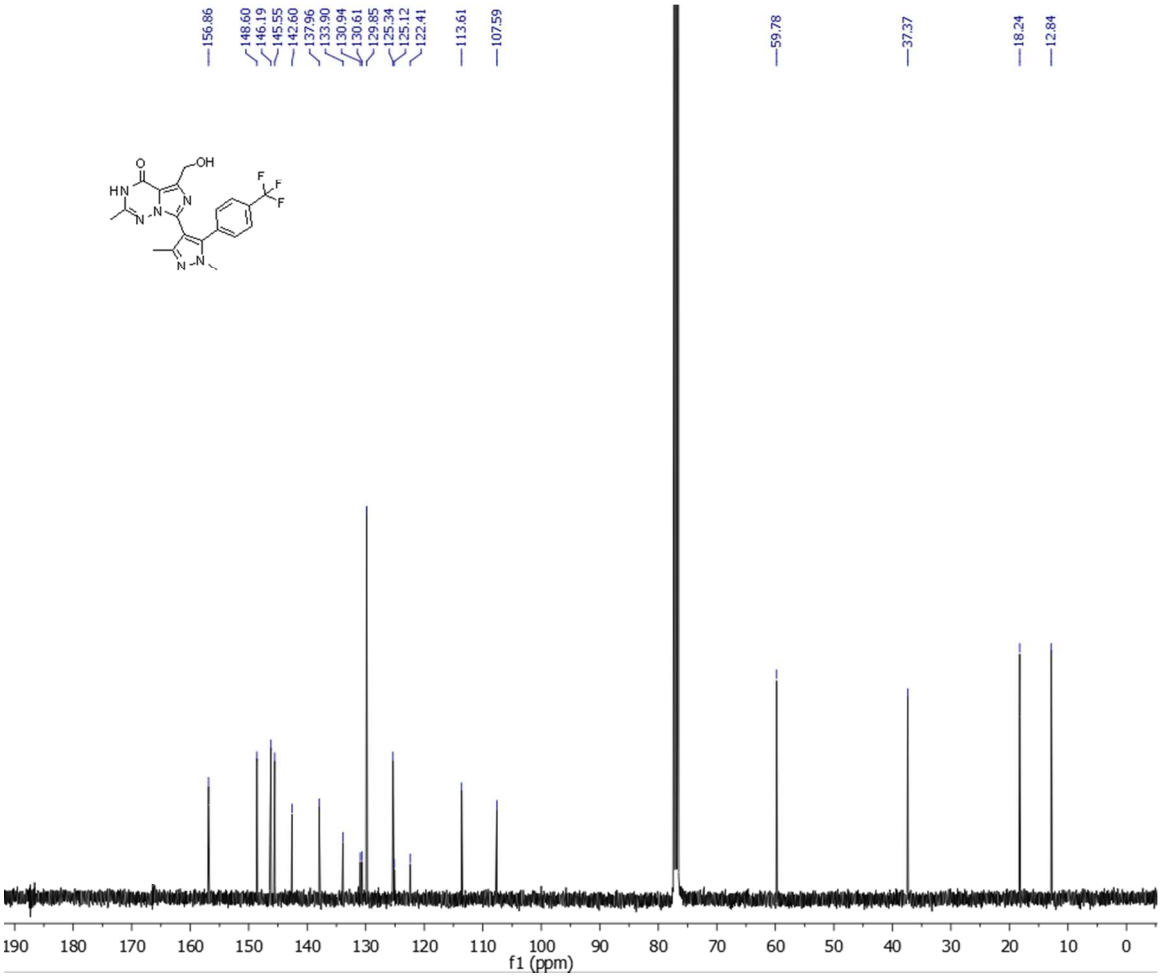

Single X-ray crystal structure of PF-06815189

- The structure was solved in the $Pca2_1$ space group
- The asymmetric unit is comprised of one molecule of PF-06815189 one molecule of water and one molecule of THF
- R value 5.9%

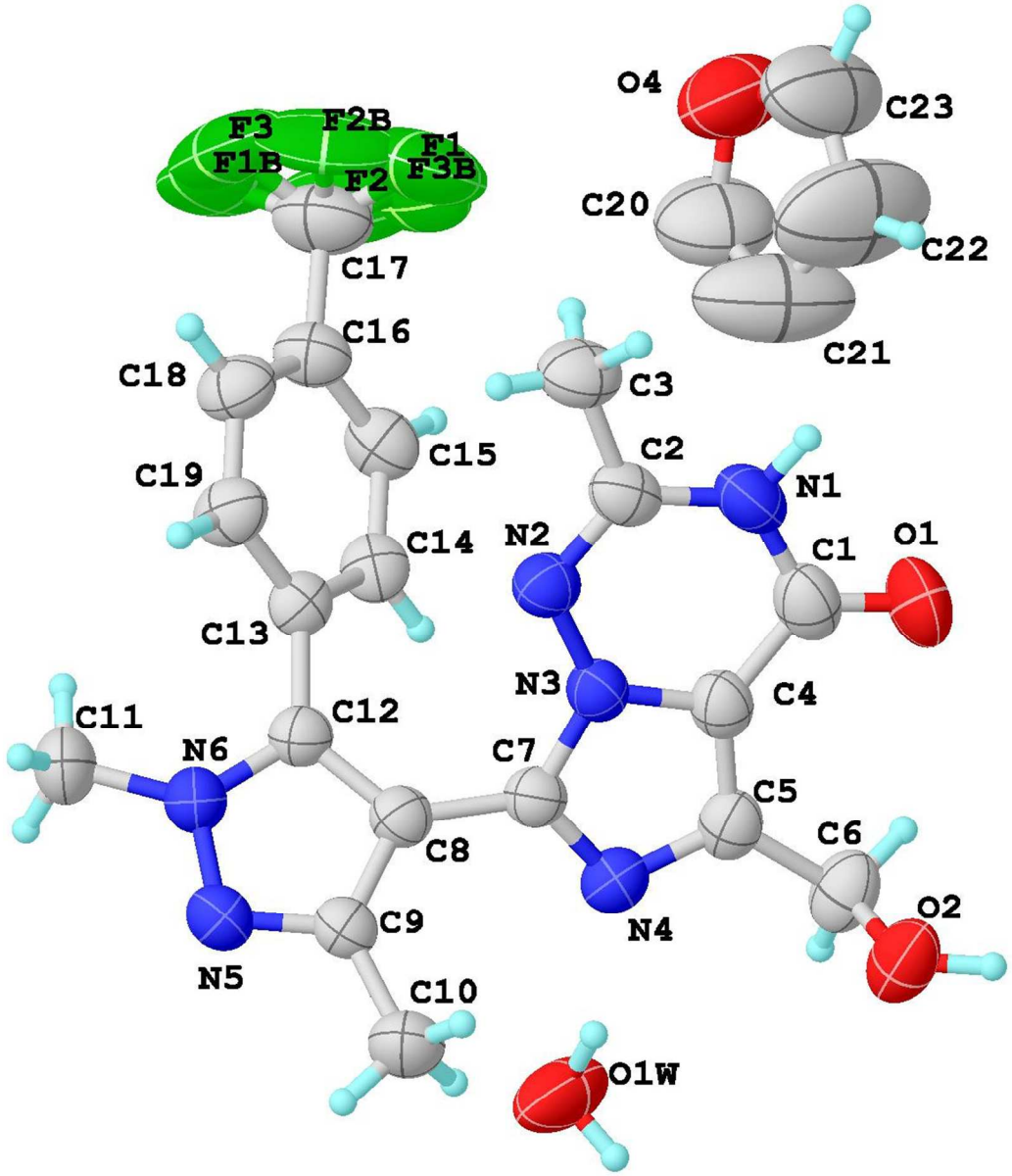

Figure. ORTEP diagram with displacement parameters drawn at 50% probability.

Experimental:

Data collection was performed on a Bruker APEX diffractometer at room temperature. Data collection consisted of omega and phi scans.
The structure was solved by direct methods using SHELX software suite in the space group $Pca2_1$. The structure was subsequently refined by the full-matrix least squares method. All non-hydrogen atoms were found and refined using anisotropic displacement parameters.

The hydrogen atoms located on nitrogen and oxygen were found from the Fourier difference map and with distances restrained. The remaining hydrogen atoms were placed in calculated positions and were allowed to ride on their carrier atoms. The final refinement included isotropic displacement parameters for all hydrogen atoms.

The CF3 group is disordered and was modeled with two occupancy positions. The THF is likely disordered in two positions, with only one occupancy shown in this structure solution; occupancy estimated at 1.

The final R-index was 5.9%. A final difference Fourier revealed no missing or misplaced electron density.

Pertinent crystal, data collection and refinement are summarized in table 1. Atomic coordinates, bond lengths, bond angles, Torsion angles and displacement parameters are listed in tables 2 –5.

Software and References
SHELXTL, Version 5.1, Bruker AXS, 1997

PLATON, A.L. Spek, J. Appl. Cryst. 2003, 36, 7-13.

MERCURY, C.F. Macrae, P.R. Edington, P. McCabe, E. Pidcock, G.P. Shields, R. Taylor, M. Towler and J. van de Streek, *J. Appl. Cryst.* **39**, 453-457, 2006.

OLEX2, Dolomanov, O.V.; Bourhis, L.J.; Gildea, R.J.; Howard, J.A.K.; Puschmann, H., (2009). J. Appl. Cryst., 42, 339-341.

Table. Crystal data and structure refinement for PF-06815189.

Identification code	z518_0m
Empirical formula	C23 H21 F3 N6 O4
Formula weight	502.46
Temperature	296(2) K
Wavelength	1.54178 Å
Crystal system	Orthorhombic
Space group	Pca2(1)
Unit cell dimensions	a = 11.6969(3) Å □= 90°. b = 12.5572(4) Å □= 90°. c = 17.2544(5) Å □ = 90°.
Volume	2534.33(13) $Å^3$
Z	4
Density (calculated)	1.317 Mg/m^3
Absorption coefficient	0.920 mm^{-1}
F(000)	1040
Crystal size	0.28 x 0.14 x 0.08 mm^3
Theta range for data collection	3.52 to 70.42°.
Index ranges	-13<=h<=11, -15<=k<=15, -21<=l<=21
Reflections collected	35037
Independent reflections	4801 [R(int) = 0.1475]
Completeness to theta = 70.42°	99.2 %
Absorption correction	None
Max. and min. transmission	0.9300 and 0.7827
Refinement method	Full-matrix least-squares on F^2
Data / restraints / parameters	4801 / 10 / 371
Goodness-of-fit on F^2	1.026
Final R indices [I>2sigma(I)]	R1 = 0.0587, wR2 = 0.1575
R indices (all data)	R1 = 0.0702, wR2 = 0.1707
Absolute structure parameter	0.3(3)
Extinction coefficient	0.0012(3)
Largest diff. peak and hole	0.303 and -0.211 $e.Å^{-3}$

Table. Atomic coordinates (x 10^4) and equivalent isotropic displacement parameters ($Å^2$x 10^3) for PF-06815189. U(eq) is defined as one third of the trace of the orthogonalized U^{ij} tensor.

	x	y	z	U(eq)
C(1)	1522(3)	5864(3)	6526(2)	67(1)
C(2)	1924(2)	6765(2)	5308(2)	56(1)
C(3)	1750(3)	7770(3)	4861(3)	75(1)

C(4)	2209(2)	5019(2)	6212(2)	54(1)
C(5)	2545(3)	4019(2)	6454(2)	55(1)
C(6)	2250(3)	3458(3)	7194(2)	69(1)
C(7)	3286(2)	4262(2)	5314(2)	48(1)
C(8)	3950(2)	4111(2)	4611(2)	50(1)
C(9)	3997(2)	3164(2)	4174(2)	50(1)
C(10)	3368(3)	2149(3)	4288(2)	72(1)
C(11)	6030(3)	4606(3)	3106(2)	76(1)
C(12)	4676(2)	4819(2)	4230(2)	50(1)
C(13)	4931(2)	5954(2)	4394(2)	50(1)
C(14)	5183(2)	6284(2)	5140(2)	54(1)
C(15)	5344(3)	7345(3)	5308(2)	61(1)
C(16)	5269(3)	8085(3)	4720(2)	62(1)
C(17)	5401(4)	9239(3)	4901(3)	95(1)
C(18)	5026(3)	7777(3)	3968(2)	66(1)
C(19)	4856(3)	6710(3)	3804(2)	61(1)
C(20)	4270(7)	9225(5)	7401(5)	136(2)
C(21)	3300(8)	8534(6)	7311(8)	183(4)
C(22)	2323(8)	9208(8)	7394(10)	220(7)
C(23)	2711(6)	10253(6)	7394(7)	171(4)
F(1)	4406(8)	9661(7)	5112(13)	171(6)
F(2)	6023(14)	9434(7)	5501(7)	143(5)
F(3)	5740(20)	9812(7)	4337(4)	185(8)
F(2B)	4770(20)	9862(10)	4488(17)	134(10)
F(3B)	5220(50)	9488(17)	5603(11)	193(18)
F(1B)	6440(13)	9565(11)	4710(30)	175(18)
N(1)	1436(2)	6718(2)	6036(2)	66(1)
N(2)	2525(2)	6017(2)	5003(2)	54(1)
N(3)	2676(2)	5146(2)	5484(1)	48(1)
N(4)	3217(2)	3566(2)	5901(1)	54(1)
N(5)	4721(2)	3269(2)	3578(2)	58(1)
N(6)	5112(2)	4284(2)	3624(2)	57(1)
O(1)	1056(3)	5849(3)	7157(2)	98(1)
O(2)	1263(3)	2824(2)	7093(1)	78(1)
O(4)	3868(3)	10263(3)	7326(3)	132(2)
O(1W)	4703(2)	1826(2)	6279(3)	105(1)

Table. Bond lengths [Å] and angles [°] for PF-06815189.

C(1)-O(1)	1.218(4)	N(1)-C(1)-C(4)	112.8(3)
C(1)-N(1)	1.368(5)	N(2)-C(2)-N(1)	124.5(3)
C(1)-C(4)	1.437(5)	N(2)-C(2)-C(3)	118.7(3)
C(2)-N(2)	1.286(4)	N(1)-C(2)-C(3)	116.7(3)
C(2)-N(1)	1.381(4)	N(3)-C(4)-C(5)	105.5(3)
C(2)-C(3)	1.493(5)	N(3)-C(4)-C(1)	118.6(3)
C(4)-N(3)	1.379(4)	C(5)-C(4)-C(1)	135.9(3)
C(4)-C(5)	1.380(5)	N(4)-C(5)-C(4)	109.5(3)
C(5)-N(4)	1.361(4)	N(4)-C(5)-C(6)	122.3(3)
C(5)-C(6)	1.499(5)	C(4)-C(5)-C(6)	128.2(3)
C(6)-O(2)	1.413(4)	O(2)-C(6)-C(5)	110.3(3)
C(7)-N(4)	1.340(4)	N(4)-C(7)-N(3)	109.9(2)
C(7)-N(3)	1.351(3)	N(4)-C(7)-C(8)	125.3(2)
C(7)-C(8)	1.454(4)	N(3)-C(7)-C(8)	124.8(2)
C(8)-C(12)	1.394(4)	C(12)-C(8)-C(9)	105.2(2)
C(8)-C(9)	1.409(4)	C(12)-C(8)-C(7)	129.5(3)
C(9)-N(5)	1.338(4)	C(9)-C(8)-C(7)	125.3(2)
C(9)-C(10)	1.485(4)	N(5)-C(9)-C(8)	110.7(2)
C(11)-N(6)	1.456(4)	N(5)-C(9)-C(10)	120.0(3)
C(12)-N(6)	1.343(4)	C(8)-C(9)-C(10)	129.3(3)
C(12)-C(13)	1.482(4)	N(6)-C(12)-C(8)	106.2(2)
C(13)-C(14)	1.385(4)	N(6)-C(12)-C(13)	123.6(3)
C(13)-C(19)	1.395(4)	C(8)-C(12)-C(13)	130.2(3)
C(14)-C(15)	1.376(5)	C(14)-C(13)-C(19)	119.2(3)
C(15)-C(16)	1.379(5)	C(14)-C(13)-C(12)	120.5(3)
C(16)-C(18)	1.383(5)	C(19)-C(13)-C(12)	120.2(3)
C(16)-C(17)	1.490(5)	C(15)-C(14)-C(13)	121.0(3)
C(17)-F(3B)	1.269(13)	C(14)-C(15)-C(16)	119.3(3)
C(17)-F(3)	1.274(7)	C(15)-C(16)-C(18)	120.9(3)
C(17)-F(2B)	1.288(11)	C(15)-C(16)-C(17)	119.7(3)
C(17)-F(2)	1.289(8)	C(18)-C(16)-C(17)	119.3(3)
C(17)-F(1B)	1.323(12)	F(3B)-C(17)-F(3)	130.0(13)
C(17)-F(1)	1.330(9)	F(3B)-C(17)-F(2B)	106.5(18)
C(18)-C(19)	1.383(5)	F(3)-C(17)-F(2B)	54.2(10)
C(20)-O(4)	1.391(7)	F(3B)-C(17)-F(2)	44.0(19)
C(20)-C(21)	1.438(11)	F(3)-C(17)-F(2)	109.2(8)
C(21)-C(22)	1.429(13)	F(2B)-C(17)-F(2)	130.7(8)
C(22)-C(23)	1.389(10)	F(3B)-C(17)-F(1B)	108(2)
C(23)-O(4)	1.358(7)	F(3)-C(17)-F(1B)	49.4(12)
N(2)-N(3)	1.385(3)	F(2B)-C(17)-F(1B)	101.6(14)
N(5)-N(6)	1.356(4)	F(2)-C(17)-F(1B)	67.6(16)
		F(3B)-C(17)-F(1)	59.6(19)
O(1)-C(1)-N(1)	122.1(3)	F(3)-C(17)-F(1)	105.1(10)
O(1)-C(1)-C(4)	125.1(4)	F(2B)-C(17)-F(1)	53.9(12)

F(2)-C(17)-F(1)	101.4(8)
F(1B)-C(17)-F(1)	138.4(7)
F(3B)-C(17)-C(16)	115.0(12)
F(3)-C(17)-C(16)	114.9(5)
F(2B)-C(17)-C(16)	114.6(7)
F(2)-C(17)-C(16)	114.2(5)
F(1B)-C(17)-C(16)	110.1(7)
F(1)-C(17)-C(16)	110.8(5)
C(16)-C(18)-C(19)	119.6(3)
C(18)-C(19)-C(13)	120.0(3)
O(4)-C(20)-C(21)	106.8(6)
C(22)-C(21)-C(20)	105.2(6)
C(23)-C(22)-C(21)	107.4(7)
O(4)-C(23)-C(22)	109.6(6)
C(1)-N(1)-C(2)	124.4(3)
C(2)-N(2)-N(3)	113.7(2)
C(7)-N(3)-C(4)	108.2(2)
C(7)-N(3)-N(2)	125.9(2)
C(4)-N(3)-N(2)	125.9(2)
C(7)-N(4)-C(5)	106.9(2)
C(9)-N(5)-N(6)	105.1(2)
C(12)-N(6)-N(5)	112.8(2)
C(12)-N(6)-C(11)	128.3(3)
N(5)-N(6)-C(11)	118.3(3)
C(23)-O(4)-C(20)	108.7(5)

Symmetry transformations used to generate equivalent atoms:

Table. Anisotropic displacement parameters ($Å^2 x\ 10^3$) for PF-06815189. The anisotropic displacement factor exponent takes the form: $-2\pi^2[\ h^2\ a^{*2}U^{11} + ...\ + 2\ h\ k\ a^*\ b^*\ U^{12}\ ]$

	U^{11}	U^{22}	U^{33}	U^{23}	U^{13}	U^{12}
C(1)	68(2)	71(2)	62(2)	-18(2)	8(2)	-6(2)
C(2)	46(1)	50(2)	73(2)	-6(1)	-4(1)	1(1)
C(3)	69(2)	60(2)	95(3)	4(2)	-3(2)	12(2)
C(4)	54(2)	58(2)	51(1)	-9(1)	4(1)	-6(1)
C(5)	59(2)	60(2)	47(1)	-4(1)	1(1)	-11(1)
C(6)	75(2)	83(2)	51(1)	4(2)	-1(1)	-17(2)
C(7)	48(1)	46(1)	51(1)	0(1)	0(1)	1(1)
C(8)	47(1)	48(1)	55(2)	1(1)	2(1)	2(1)
C(9)	51(1)	47(1)	53(1)	-2(1)	3(1)	5(1)
C(10)	82(2)	54(2)	79(2)	-7(2)	10(2)	-5(2)
C(11)	79(2)	74(2)	76(2)	-1(2)	31(2)	-1(2)
C(12)	51(2)	46(1)	54(2)	2(1)	2(1)	2(1)
C(13)	46(1)	51(1)	52(1)	2(1)	-2(1)	0(1)
C(14)	52(2)	60(2)	51(1)	4(1)	-7(1)	5(1)
C(15)	62(2)	66(2)	56(2)	-8(1)	-10(1)	2(1)
C(16)	69(2)	52(2)	66(2)	-6(1)	-7(1)	0(1)
C(17)	125(4)	58(2)	101(3)	-12(2)	-16(3)	1(2)
C(18)	82(2)	56(2)	61(2)	10(1)	-7(2)	-3(1)
C(19)	74(2)	58(2)	52(2)	2(1)	-6(1)	-7(1)
C(20)	132(5)	100(4)	175(7)	14(4)	-21(5)	17(3)
C(21)	147(6)	96(4)	305(14)	0(6)	-78(8)	6(4)
C(22)	118(6)	143(7)	400(20)	31(10)	-13(9)	-41(5)
C(23)	102(4)	108(4)	303(13)	8(6)	48(6)	18(3)
F(1)	188(7)	75(4)	251(17)	-38(7)	14(9)	34(4)
F(2)	223(11)	82(4)	126(8)	-21(5)	-66(7)	-41(6)
F(3)	380(20)	77(6)	101(4)	-3(3)	33(9)	-83(11)
F(2B)	169(17)	58(6)	176(19)	7(9)	-69(15)	35(9)
F(3B)	380(50)	92(10)	104(12)	-44(9)	80(20)	0(20)
F(1B)	109(10)	51(6)	370(50)	-42(14)	38(13)	-24(5)
N(1)	65(2)	58(1)	76(2)	-15(1)	9(1)	6(1)
N(2)	49(1)	50(1)	63(1)	3(1)	0(1)	3(1)
N(3)	47(1)	47(1)	50(1)	-3(1)	1(1)	0(1)
N(4)	55(1)	52(1)	56(1)	4(1)	-1(1)	-4(1)
N(5)	64(1)	53(1)	58(1)	-6(1)	6(1)	3(1)
N(6)	60(1)	53(1)	57(1)	1(1)	10(1)	1(1)
O(1)	126(2)	96(2)	73(2)	-20(2)	42(2)	4(2)
O(2)	102(2)	80(2)	53(1)	-8(1)	7(1)	-36(1)
O(4)	106(3)	89(2)	201(5)	34(3)	20(3)	-1(2)
O(1W)	68(2)	73(2)	173(3)	41(2)	21(2)	1(1)

Phosphodiesterase PDE2A1 Data

		IC50 (nM)						GeoMean IC50		Mean pIC50	SD	SEM
		N=1	N=2	N=3	N=4	N=5		(nM)				
	5	6.68	6.80	7.23	7.01	-		6.93		8.16	0.01	0.01
	6	8.38	7.95	8.00	7.08	-		7.84		8.11	0.03	0.02
	PF-06815189	0.31	0.32	0.33	0.34	1.08		0.41		9.38	0.23	0.10

	PDE2A1 IC50 (nM)								GeoMean IC50		Mean pIC50	SD	SEM
	N=1	N=2	N=3	N=4	N=5	N=6	N=7		(nM)				
1	0.59	0.55	0.46	0.55	0.71	1.00	-		0.62		9.21	0.12	0.05
BAY 60-7550	0.33	0.36	0.04	0.36	0.24	0.36	0.17		0.22		9.66	0.12	0.05

Phosphodiesterase PDE2A1 Assay

The human phosphodiesterase (PDE) 2A1 assay measures the conversion of 3', 5'-[^{3}H] cGMP to 5'-[^{3}H]. Yttrium silicate (YSi) scintillation proximity (SPA) beads bind selectively to 5'-[^{3}H] GMP, with the magnitude of radioactive counts being directly related to PDE enzymatic activity. The assay was performed in white walled opaque bottom 384-well plates. 0.5 µL of compound in dimethyl sulfoxide was added to each well. Enzyme (15 µL) was then added to each well in buffer (in mM: Trizma, 50 (pH7.5); $MgCl_2$, 1.3 mM) containing Brij 35 (0.01% (v/v)). Subsequently, 10 µl of 3',5'-[^{3}H] cGMP (125 nM) was added to each well to start the reaction and the plates were incubated for 30 minutes at 25^{o}C. The reaction was terminated by the addition of 10 µl of PDE YSi SPA beads (Perkin Elmer). Following an additional 1 hour incubation period the plates were read on a MicroBeta radioactive plate counter (Perkin Elmer, Waltham. MA) to determine radioactive counts per well.

Data Analysis

Inhibition curves were plotted from individual experiments, and IC_{50} values were determined using a four parameter logistic fit. IC_{50} is defined as the concentration of the test article that produced a 50% inhibition of a maximal response.

PDE selectivity profile of 1, PF-06815189, 5 and 6

		PDE1B1	PDE2A1	PDE3A1	PDE4D3	PDE5A1	Bovine PDE6	PDE7B	PDE8B	PDE9A1	PDE10A1	PDE11A4
Compound		**PDE Subtype IC50 (nM)**										
5	N=1	>5000	-	>5000	>5000	>5000	>5000	>5000	>5000	>5000	>5000	>5000
	N=2	>5000	-	>5000	>5000	>5000	>5000	>5000	>5000	>5000	>5000	>5000
	N=3	>5000	-	>5000	>5000	>5000	>5000	>5000	>5000	>5000	>5000	>5000
	GeoMean	**>5000**	**-**	**>5000**	**>5000**	**>5000**	**>5000**	**>5000**	**>5000**	**>5000**	**>5000**	**>5000**
6	N=1	>5000	-	>5000	>5000	>5000	>5000	>5000	>5000	>5000	>5000	>5000
	N=2	>5000	-	>5000	>5000	>5000	>5000	>5000	>5000	>5000	>5000	>5000
	GeoMean	**>5000**	**-**	**>5000**	**>5000**	**>5000**	**>5000**	**>5000**	**>5000**	**>5000**	**>5000**	**>5000**
PF-06815189	N=1	>5000	-	>5000	>5000	3060.22	>5000	>5000	>5000	>5000	>5000	>5000
	N=2	>5000	-	>5000	>5000	2015.46	>5000	>5000	>5000	>5000	>5000	>5000
	N=3	>5000	-	>5000	>5000	2351.04	>5000	>5000	>5000	>5000	>5000	>5000
	GeoMean	**>5000**	**-**	**>5000**	**>5000**	**2438.54**	**>5000**	**>5000**	**>5000**	**>5000**	**>5000**	**>5000**
1	N=1	1710.00	-	6230.00	>30000	1570.00	3870.00	2070.00	>30000	>30000	1220.00	>30000
	N=2	1730.00	-	707.00	>30000	474.00	3050.00	2330.00	>30000	>30000	3580.00	>30000
	N=3		-	6210.00	>30000	494.00						
	N=4		-			442.00						
	N=5		-									
	N=6		-									
	N=7		-									
	GeoMean (nM)	**1720.64**	**-**	**3027.39**	**>30000**	**635.34**	**3437.40**	**2199.41**	**>30000**	**>30000**	**2087.87**	**>30000**

PDE Methods

Phosphodiesterase Assays

The phosphodiesterase (PDE) assays measure the conversion of 3', 5'-[^{3}H] cAMP to 5'-[^{3}H] AMP (for PDE 1B1, 3A1, 4D3, 7B, 8B and 10A1) or 3', 5'-[^{3}H] cGMP to 5'-[^{3}H] GMP (for PDE 2A1, 5A1, 6, 9A1 and 11A4) by the relevant PDE enzyme subtype. Yttrium silicate (YSi) scintillation proximity (SPA) beads bind selectively to 5'-[^{3}H] AMP or 5'-[^{3}H] GMP, with the magnitude of radioactive counts being directly related to PDE enzymatic activity. The assay is performed in white walled opaque bottom 384-well plates. 1 µl of compound in dimethyl sulfoxide is added to each well. Enzyme solution is then added to each well in buffer (in mM: Trizma, 50 (pH7.5); $MgCl_2$, 1.3 mM) containing Brij 35 (0.01% (v/v)). For PDE1 subtype assays the buffer additionally included $CaCl_2$ (30 mM) and calmodulin (25 U/ml). Subsequently, 20 µl of 3',5'-[^{3}H] cGMP (125 nM) or 20 µL of 3',5'-[^{3}H] cAMP (50 nM) is added to each well to start the reaction and the plate is incubated for 30 minutes at 25^{o}C. The reaction is terminated by the addition of 20 µl of PDE YSi SPA beads (Perkin Elmer). Following an additional 8 hour incubation period the plates are read on a MicroBeta radioactive plate counter (Perkin Elmer) to determine radioactive counts per well.

Data Analysis

Inhibition curves are plotted from individual experiments, and IC_{50} values were determined using a four parameter logistic fit. IC_{50} is defined as the concentration of the test article that produced a 50% inhibition of a maximal response.

Off-target profile of PF-06815189

Overview of PF-06815189 Pharmacology

PF-06815189 was profiled against a broad panel of phosphodiesterase (PDE) suptypes that included PDEs 1 through 11. As shown in the Table above, PF-06815189 was highly selective for PDE2A1 with an IC_{50} value of 0.41 nM. Significantly weaker activity was also observed at PDE5A1 (IC_{50} = 1.77 μM), PDE1B1 (IC_{50} = 5.26 μM) PDE3A1 (IC_{50} = 11.80 μM) and PDE10A1 (IC_{50} = 20.36 μM). For all other PDE subtypes the IC_{50} value was greater than 30 μM.

To determine the selectivity of PF-06815189 against a wider diversity of targets profiling was performed against a panel of 66 targets that included GPCRs, ion channels, amine transporters, enzymes and kinases at Eurofins Cerep SA (Celle L'Evescault, France). A single activity was observed, against the muscarinic M2 receptor, where the compound appeared to show antagonist activity with a K_b value of 18 nM in a functional assay that measured cAMP as an endpoint. The potential arose that this activity was therefore an artifact due to PDE2 inhibition in the recombinant cell line used in the assay. To further evaluate this activity, PF-06815189 was also profiled in an M2 binding assay and an M2 beta arrestin functional assay, assays that would not be susceptible to interference due to PDE inhibition. No M2 activity was observed in either assay, strongly suggesting that the initial M2 was indeed an artifact. Hence overall the PF-06815189 displayed an excellent selectively profile with respect to its PDE2 activity.

Data from other select off-targets:

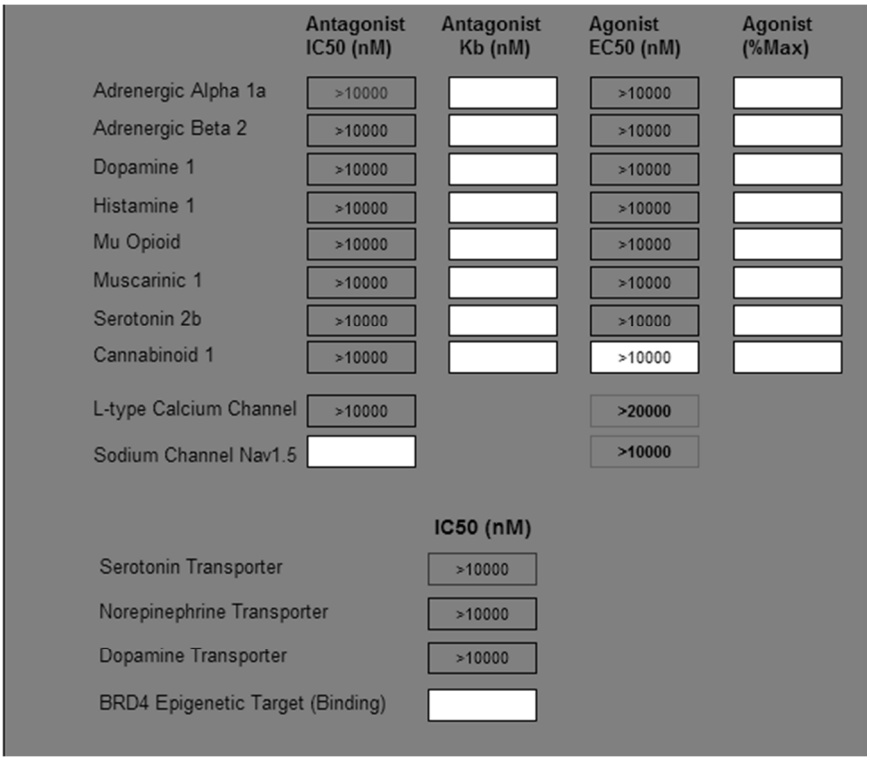

	Antagonist IC50 (nM)	Antagonist Kb (nM)	Agonist EC50 (nM)	Agonist (%Max)
Adrenergic Alpha 1a	>10000		>10000	
Adrenergic Beta 2	>10000		>10000	
Dopamine 1	>10000		>10000	
Histamine 1	>10000		>10000	
Mu Opioid	>10000		>10000	
Muscarinic 1	>10000		>10000	
Serotonin 2b	>10000		>10000	
Cannabinoid 1	>10000		>10000	
L-type Calcium Channel	>10000		>20000	
Sodium Channel Nav1.5			>10000	

	IC50 (nM)
Serotonin Transporter	>10000
Norepinephrine Transporter	>10000
Dopamine Transporter	>10000
BRD4 Epigenetic Target (Binding)	

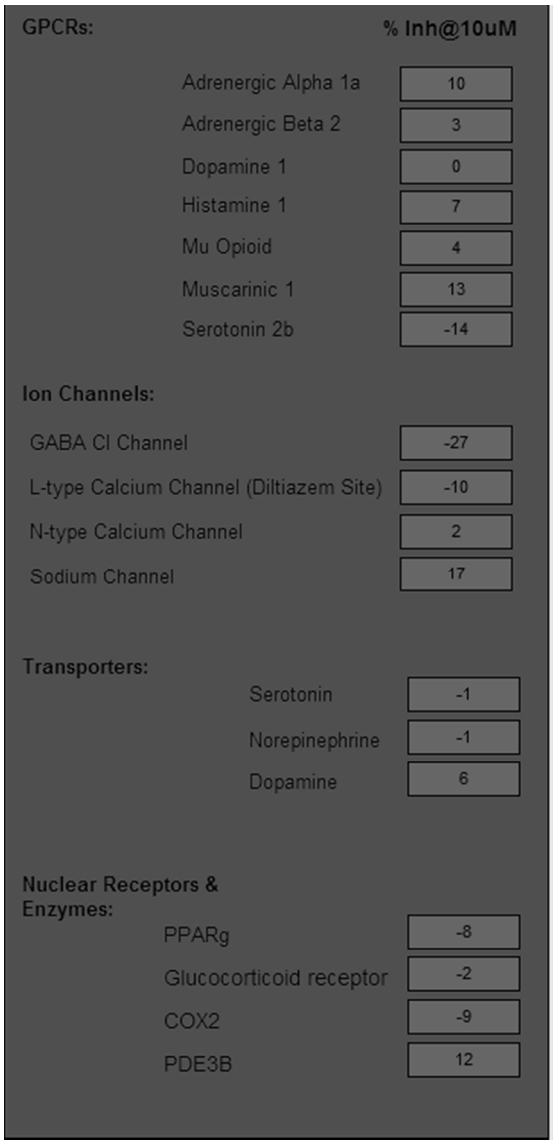

GPCRs:	% Inh@10uM
Adrenergic Alpha 1a	10
Adrenergic Beta 2	3
Dopamine 1	0
Histamine 1	7
Mu Opioid	4
Muscarinic 1	13
Serotonin 2b	-14
Ion Channels:	
GABA Cl Channel	-27
L-type Calcium Channel (Diltiazem Site)	-10
N-type Calcium Channel	2
Sodium Channel	17
Transporters:	
Serotonin	-1
Norepinephrine	-1
Dopamine	6
Nuclear Receptors & Enzymes:	
PPARg	-8
Glucocorticoid receptor	-2
COX2	-9
PDE3B	12

Procedure for Miles assay with PF-06815189

Rat studies were done at BioDuro, Pharmaceutical Product Development Inc. (Shanghai, PRC); animal care and *in vivo* procedures were conducted according to guidelines from the BioDuro Institutional Animal Care and Use Committee.

Animals: guinea pigs, male, 250 ~ 300 g, n=2 per group.

Study Design: Animal flank skin hair is clipped and depilated one day before permeability experiments. Animals are anesthetized, and injected with 0.5 mLof 0.5% filtered Evans Blue (EB, Sigma) via the left femoral vein. After the animals regain consciousness histamine (500 ng) was administered in a volume of 0.1 mL and injected intradermally into flank skin. Twenty minutes after trigger exposure, animal skin lesions are harvested. The sampled skin is incubated in formamide solution at 70 C for 48 hours. The EB extract is ultra-centrifuged and processed to measure the absorbance at 620 nm and 740 nm using a spectrophotometer.

Dosing: PF-06815189 was administered *s.c.* and was diluted in 30%PEG400 and 70% SBECD 20%. Compound or vehicle was dosed 30 minutes before administration of Evan's Blue dye.

Recombinant CYP (rCYP) assay procedure

Metabolic Lability in recombinant Human Cytochrome P450 Enzymes. Compounds (1 uM) were incubated with microsomes containing heterologously expressed human P450 enzymes (100 pmol/mL) in a volume of 0.015 mL of potassium phosphate buffer (100 mM, pH 7.4) containing MgCl2 (3 mM) and NADPH (2 mM). Incubations were commenced with the addition of NADPH and carried out at 37oC. At time points of 0, 3, 5, 10, 20, 30, and 60 min, incubations were terminated by addition of acetonitrile (0.06 mL) containing an internal standard ((E)-3-(4-(((2S,3S,4S,5R)-5-((E)-1-(((3-chloro-2,6-difluorobenzyl)oxy)imino)ethyl)-3,4-dihydroxytetrahydrofuran-2-yl)oxy)-3-hydroxyphenyl)-2-methyl-N-((3aS,4R,5R,6S,7R,7aR)-4,6,7-trihydroxyhexahydrobenzo[d][1,3]dioxol-5-yl)acrylamide; 100 ng/mL). The terminated incubation mixtures were spun in a centrifuge at 1200g for 10 min, and the supernatant was mixed with two volumes of water for analysis by HPLC-MS.

Recombinant CYP (rCYP) assay data for 1

rCYP1A2 $CL_{int, app}$ < 0.038 µl/min/pmol
rCYP2B6 $CL_{int, app}$ < 0.038 µl/min/pmol
rCYP2C19 $CL_{int, app}$ < 0.038 µl/min/pmol
rCYP2C8 $CL_{int, app}$ < 0.038 µl/min/pmol
rCYP2C9 $CL_{int, app}$ < 0.038 µl/min/pmol
rCYP2D6 $CL_{int, app}$ < 0.038 µl/min/pmol
rCYP3A4 $CL_{int, app}$ = 1.93 µl/min/pmol

Compound 1 iv/po rat PK

Rat studies were done at BioDuro, Pharmaceutical Product Development Inc. (Shanghai, PRC); animal care and *in vivo* procedures were conducted according to guidelines from the BioDuro Institutional Animal Care and Use Committee. Jugular vein cannulated male Wistar-Han rats (~250 g), obtained from Vital River (Beijing, China) were used for these studies. Rats were provided *ad libitum* access to water and food. **1** was administered intravenously (i.v.) in 10% DMSO/30% PEG 400/60% water via the tail vein of rats at a dose of 1.0 mg/kg in a dosing volume of 1 ml/kg or by oral gavage in 0.5% methylcellulose in water at a dose of 3.0 mg/kg in a dosing volume of 5 mL/kg. Serial blood samples were collected from the jugular vein before dosing and 0.033, 0.083, 0.25, 0.5, 1, 2, 4, 7, and 24 h after dosing. Blood samples from the pharmacokinetic studies were centrifuged to generate plasma. All plasma samples were kept frozen until analysis. Urine samples (0–7.0 and 7.0–24 h) were also collected after i.v. administration. Aliquots of plasma or urine were transferred to 96-well blocks and methanol/acetonitrile containing an internal standard was added to each well. Samples were then analyzed by LC-MS/MS and concentrations of **1** in plasma and urine were determined by interpolation from a standard curve.

PF-06815189 iv/po PK in rat

Rat studies were done at BioDuro, Pharmaceutical Product Development Inc. (Shanghai, PRC); animal care and *in vivo* procedures were conducted according to guidelines from the BioDuro Institutional Animal Care and Use Committee. Jugular vein cannulated male Wistar-Han rats (~250 g), obtained from Vital River (Beijing, China) were used for these studies. Rats were provided *ad libitum* access to water and food. PF-06815189 was administered intravenously (i.v.) in 10% DMSO/30% PEG 400/60% water via the tail vein of rats at a dose of 1.0 mg/kg in a dosing volume of 1 ml/kg or by oral gavage in 0.5% methylcellulose in water at a dose of 5.0 mg/kg in a dosing volume of 5 mL/kg. Serial blood samples were collected from the jugular vein before dosing and 0.033, 0.083, 0.25, 0.5, 1, 2, 4, 7, and 24 h after dosing. Blood samples from the pharmacokinetic studies were centrifuged to generate plasma. All plasma samples were kept frozen until analysis. Urine samples (0–7.0

and 7.0–24 h) were also collected after i.v. administration. Aliquots of plasma or urine were transferred to 96-well blocks and methanol/acetonitrile containing an internal standard was added to each well. Samples were then analyzed by LC-MS/MS and concentrations of PF-06815189 in plasma and urine were determined by interpolation from a standard curve.

PF-06815189 iv/po PK in dog

Dog experiments were conducted in our AAALAC-accredited facilities and were reviewed and approved by Pfizer Institutional Animal Care and Use Committee. Male Beagle dogs (~ 8-11 kg) were used for these studies. PF-06815189 was administered intravenously (i.v.) in 10% DMSO/60% PEG 400/30% water via the cephalic vein at a dose of 1.0 mg/kg in a dosing volume of 0.2 ml/kg or by oral gavage in 0.5% methylcellulose in water at a dose of 1.0 mg/kg in a dosing volume of 1.0 mL/kg. Serial blood samples were collected from the jugular vein before dosing and 0.033, 0.083, 0.25, 0.5, 1, 2, 4, 7, and 24 h after IV dosing and at 0.25, 0.5, 1, 2, 4, 7 and 24 h after oral dosing. Blood samples from the pharmacokinetic studies were centrifuged to generate plasma. All plasma samples were kept frozen until analysis. Urine samples (0–7.0 and 7.0–24 h) were also collected after i.v. administration. Aliquots of plasma or urine were transferred to 96-well blocks and methanol/acetonitrile containing an internal standard was added to each well. Samples were then analyzed by LC-MS/MS and concentrations of PF-06815189 in plasma and urine were determined by interpolation from a standard curve.

PF-06815189 iv/po PK in NHP

NHP experiments were conducted in our AAALAC-accredited facilities and were reviewed and approved by Pfizer Institutional Animal Care and Use Committee. Male Cynomolgus monkeys (~ 4-8 kg) were used for these studies. PF-06815189 was administered intravenously (i.v.) in 10% DMSO/60% PEG 400/30% water via the cephalic vein at a dose of 1.0 mg/kg in a dosing volume of 0.2 ml/kg or by oral gavage in 0.5% methylcellulose in water at a dose of 1.0 mg/kg in a dosing volume of 1.0 mL/kg. Serial blood samples were collected from the femoral vein before dosing and 0.033, 0.083, 0.25, 0.5, 1, 2, 4, 7, and 24 h after IV dosing and at 0.25, 0.5, 1, 2, 4, 7 and 24 h after oral dosing. Blood samples from the pharmacokinetic studies were centrifuged to generate plasma. All plasma samples were kept frozen until analysis. Urine samples (0–7.0 and 7.0–24 h) were also collected after i.v. administration. Aliquots of plasma or urine were transferred to 96-well blocks and methanol/acetonitrile containing an internal standard was added to each well. Samples were then analyzed by LC-MS/MS and concentrations of PF-06815189 in plasma and urine were determined by interpolation from a standard curve.

Determination of Pharmacokinetic Parameters. Pharmacokinetic parameters were determined using noncompartmental analysis (Watson v.7.4, Thermo Scientific, Waltham, MA). The area under the plasma concentration-time curve from $t = 0$ to 24 h ($AUC_{0\text{-}24}$) and $t = 0$ to infinity ($AUC_{0\text{-}\infty}$) was estimated using the linear trapezoidal rule and CL_p was calculated as the intravenous dose divided by $AUC_{0-\infty}^{i.v.}$. The terminal rate constant (k_{el}) was calculated by a linear regression of the log-linear concentration-time curve, and the terminal elimination $t_{1/2}$ was calculated as 0.693 divided by k_{el}. Apparent steady state distribution volume (Vd_{ss}) was determined as the i.v. dose divided by the product of $AUC_{0-\infty}$ and k_{el}. Percentage of unchanged compound excreted in urine over 24 h was calculated using the following equation: amount (in mg) in urine over the 24 h interval post dose/actual amount of the dose administered (mg) x 100%.

References for Table 1

TPSA is calculated using the Topological Polar Surface Area algorithm.[8]
Intrinsic scaled clearance from human liver microsomes and hepatocytes.[9]

PF-06815189 rat exploratory toxicology study

Wistar Han rats (obtained from Charles River, 125–300 g, 6–9 weeks old at study start; n=3/sex) received once daily oral dosing of test compound or vehicle at the indicated concentrations for 15-days. The objectives of the study were to evaluate the potential tolerability, toxicokinetics, as well as the potential for micronuclei induction of PF-06815189. The doses were prepared in a solution of 0.5% methylcellulose and delivered in a volume of 10 mL/kg per day. Blood samples for bioanalytical analysis were collected in K_2EDTA tubes via jugular vessel. Plasma was isolated after centrifugation and stored at −20 °C prior to analysis. Following completion of dosing, animals were sacrificed by gas anesthesia (isoflurane) followed by exsanguination, and a standard set of tissues underwent histological examination. Results are shown in brief in the table below and include overall male/female toxicokinetic data (day 13). The test compound was negative for micronuclei formation in blood reticulocytes. Animal Welfare Compliance Statement: this study was conducted in accordance with the current guidelines for animal welfare (National Research Council Guide for the Care and Use of Laboratory Animals, 2011). The procedures used in this study have been reviewed and approved by Pfizer's Institutional Animal Care and Use Committee.

Tabular Summary: PF-06815189 rat exploratory toxicology study

Dose (mg/kg/day)	Overall Cmax (ng/mL)	Overall AUC_{24} (ng.h/mL)	Observations related to PF-06815189 treatment (↑=increase; ↓=decrease)
5	658	2180	• ↓body weight and food consumption • ↓red blood cells, hemoglobin, hematocrit; ↓alkaline phosphatase
20	5650	20000	• same as above plus: • ↓fibrinogen; ↑cholesterol • histopathology: minimal stomach multifocal erosions (1 rat)
50	7090	30800	• same as above plus: • ↑white blood cells, lymphocytes, large unstained cells • ↑liver weight (no histological correlate)

PF-06815189 dog exploratory toxicology study

Naive male beagle dogs (Canis lupus familiaris, >8 months old; n=1/sex at low and high doses; n=3/sex at mid dose) received once daily oral dosing of test compound or vehicle for 14-days at the indicated concentrations. The doses were prepared in a solution of 0.5% methylcellulose and delivered in a volume of 5 mL/kg per day. Electrocardiograms were performed on all dogs predose and approximately 1 hour postdose on dosing day 11. Blood samples for bioanalytical analysis were collected in K_2EDTA tubes via jugular vessel. Plasma was isolated after centrifugation and stored at –20 °C before analysis. Following completion of dosing, animals were sacrificed via intravenous administration of barbiturate followed by exsanguination, and a standard set of tissues underwent histological examination. Results are shown in brief in the table below and include overall male/female toxicokinetic data (day 14). Animal Welfare Compliance Statement: this study was conducted in accordance with the current guidelines for animal welfare (National Research Council Guide for the Care and Use of Laboratory Animals, 2011). The procedures used in this study have been reviewed and approved by Pfizer's Institutional Animal Care and Use Committee.

Tabular Summary: PF-06815189 dog exploratory toxicology study

Dose (mg/kg/day)	Overall Cmax (ng/mL)	Overall AUC_{24} (ng.h/mL)	Observations related to PF-06815189 treatment (↑=increase; ↓=decrease)
1	1990	11000	• cage licking and biting • ↑heart rate (1 hour postdose compared to predose)
3	8920	56100	• same as above plus: • emesis • ↓PR interval, ↓QT interval • histopathology: minimal lung arteriopathy (1 dog)
9	18600	171000	• same as above (excluding lung arteriopathy) plus: • discolored (red) eyes and gums, warm to touch, ↓activity • histopathology: minimal heart arteriopathy (1 dog); minimal atrium multifocal subepicardial fibroplasia, edema, and inflammatory cell infiltrates

References for Supporting Information

1. Helal, C. J.; Arnold, E. P.; Boyden, T. L.; Chang, C.; Chappie, T. A.; Fennell, K. F.; Forman, M. D.; Hajos, M.; Harms, J. F.; Hoffman, W. E.; Humphrey, J. M.; Kang, Z.; Kleiman, R. J.; Kormos, B. L.; Lee, C.-W.; Lu, J.; Maklad, N.; McDowell, L.; Mente, S.; O'Connor, R. E.; Pandit, J.; Piotrowski, M.; Schmidt, A. W.; Schmidt, C. J.; Ueno, H.; Verhoest, P. R.; Yang, E. X., Application of Structure-Based Design and Parallel Chemistry to Identify a Potent, Selective, and Brain Penetrant Phosphodiesterase 2A Inhibitor. *Journal of Medicinal Chemistry* **2017,** *60* (13), 5673-5698.
2. Grimme, S.; Antony, J.; Ehrlich, S.; Krieg, H., A consistent and accurate ab initio parametrization of density functional dispersion correction (DFT-D) for the 94 elements H-Pu. *Journal of Chemical Physics* **2010,** *132* (15), 154104/1-154104/19.
3. Zhao, Y.; Truhlar, D. G., The M06 suite of density functionals for main group thermochemistry, thermochemical kinetics, noncovalent interactions, excited states, and transition elements: two new functionals and systematic testing of four M06-class functionals and 12 other functionals. *Theoretical Chemistry Accounts* **2008,** *120* (1-3), 215-241.
4. Bochevarov, A. D.; Harder, E.; Hughes, T. F.; Greenwood, J. R.; Braden, D. A.; Philipp, D. M.; Rinaldo, D.; Halls, M. D.; Zhang, J.; Friesner, R. A., Jaguar: A high-performance quantum chemistry software program with strengths in life and materials sciences. *International Journal of Quantum Chemistry* **2013,** *113* (18), 2110-2142.
5. Helal, C. J.; Arnold, E. P.; Boyden, T. L.; Chang, C.; Chappie, T. A.; Fennell, K. F.; Forman, M. D.; Hajos, M.; Harms, J. F.; Hoffman, W. E.; Humphrey, J. M.; Kang, Z.; Kleiman, R. J.; Kormos, B. L.; Lee, C.-W.; Lu, J.; Maklad, N.; McDowell, L.; Mente, S.; O'Connor, R. E.; Pandit, J.; Piotrowski, M.; Schmidt, A. W.; Schmidt, C. J.; Ueno, H.; Verhoest, P. R.; Yang, E. X., Application of Structure-Based Design and Parallel Chemistry to Identify a Potent, Selective, and Brain Penetrant Phosphodiesterase 2A Inhibitor. *Journal of Medicinal Chemistry* **2017**, *J. Med. Chem.* **2017**, 60, 5673-5698.
6. (a) Friesner, R. A.; Murphy, R. B.; Repasky, M. P.; Frye, L. L.; Greenwood, J. R.; Halgren, T. A.; Sanschagrin, P. C.; Mainz, D. T., Extra Precision Glide: Docking and Scoring Incorporating a Model of Hydrophobic Enclosure for Protein-Ligand Complexes. *Journal of Medicinal Chemistry* **2006,** *49* (21), 6177-6196; (b) Halgren, T. A.; Murphy, R. B.; Friesner, R. A.; Beard, H. S.; Frye, L. L.; Pollard, W. T.; Banks, J. L., Glide: A new approach for rapid, accurate docking and scoring. 2. Enrichment factors in database screening. *Journal of Medicinal Chemistry* **2004,** *47* (7), 1750-1759; (c) Friesner, R. A.; Banks, J. L.; Murphy, R. B.; Halgren, T. A.; Klicic, J. J.; Mainz, D. T.; Repasky, M. P.; Knoll, E. H.; Shelley, M.; Perry, J. K.; Shaw, D. E.; Francis, P.; Shenkin, P. S., Glide: A new approach for rapid, accurate docking and scoring. 1. method and assessment of docking accuracy. *Journal of Medicinal Chemistry* **2004,** *47* (7), 1739-1749.
7. Madhavi Sastry, G.; Adzhigirey, M.; Day, T.; Annabhimoju, R.; Sherman, W., Protein and ligand preparation: parameters, protocols, and influence on virtual screening enrichments. *Journal of Computer-Aided Molecular Design* **2013,** *27* (3), 221-234.
8. Ertl, P.; Rohde, B.; Selzer, P., Fast Calculation of Molecular Polar Surface Area as a Sum of Fragment-Based Contributions and Its Application to the Prediction of Drug Transport Properties. *Journal of Medicinal Chemistry* **2000,** *43* (20), 3714-3717.
9. Hosea, N. A.; Collard, W. T.; Cole, S.; Maurer, T. S.; Fang, R. X.; Jones, H.; Kakar, S. M.; Nakai, Y.; Smith, B. J.; Webster, R.; Beaumont, K., Prediction of human pharmacokinetics from preclinical information: comparative accuracy of quantitative prediction approaches. *Journal of Clinical Pharmacology* **2009,** *49* (5), 513-533.